

1 In review for a journal publication

2

3 **Short-range airborne route dominates exposure of respiratory**  
4 **infection during close contact**

5

6 **Wenzhao Chen<sup>1</sup>, Nan Zhang<sup>1</sup>, Jianjian Wei<sup>3</sup>, Hui-Ling Yen<sup>2</sup>, Yuguo Li<sup>1,2,\*</sup>**

7

8 1 Department of Mechanical Engineering, The University of Hong Kong, Pokfulam Road,  
9 Hong Kong, China

10 2 School of Public Health, The University of Hong Kong, 7 Sassoon Road, Pokfulam,  
11 Hong Kong, China

12 3 Institute of Refrigeration and Cryogenics/Key Laboratory of Refrigeration and Cryogenic  
13 Technology of Zhejiang Province, Zhejiang University, Hangzhou, China

14

15 \* Corresponding author:

16 Yuguo Li

17 Department of Mechanical Engineering, The University of Hong Kong, Pokfulam  
18 Road, Hong Kong, China

19 Email address: liyg@hku.hk

20 Telephone number: +852 3917 2625

21 Fax: +952 2858 5415

22

23 **Abstract**

24 A susceptible person experiences the highest exposure risk of respiratory infection when he  
25 or she is in close proximity with an infected person. The large droplet route has been  
26 commonly believed to be dominant for most respiratory infections since the early 20<sup>th</sup>  
27 century, and the associated droplet precaution is widely known and practiced in hospitals and  
28 in the community. The mechanism of exposure to droplets expired at close contact, however,  
29 remains surprisingly unexplored. In this study, the exposure to exhaled droplets during close  
30 contact (< 2 m) via both the short-range airborne and large droplet sub-routes is studied using  
31 a simple mathematical model of expired flows and droplet dispersion/deposition/inhalation,  
32 which enables the calculation of exposure due to both deposition and inhalation. The short-  
33 range airborne route is found to dominate at most distances studied during both talking and  
34 coughing. The large droplet route only dominates when the droplets are larger than 100  $\mu\text{m}$   
35 and when the subjects are within 0.2 m while talking or 0.5 m while coughing. The smaller  
36 the exhaled droplets, the more important the short-range airborne route. The large droplet  
37 route contributes less than 10% of exposure when the droplets are smaller than 50  $\mu\text{m}$  and  
38 when the subjects are more than 0.3 m apart, even while coughing.

39 **Keywords:** exposure, disease transmission, close contact, short-range airborne, large droplet

40 **Practical implications**

41 Our simple but novel analysis shows that conventional surgical masks are not effective if most  
42 infectious viruses are contained in fine droplets, and non-conventional intervention methods  
43 such as personalised ventilation should be considered as infection prevention strategies given  
44 the possible dominance of the short-range airborne route, although further clinical evidence is  
45 needed.

46

47 **Nomenclature**

NOTE: This preprint reports new research that has not been certified by peer review and should not be used to guide clinical practice.

48

49 Subscript

50

- $i$  Droplets of different diameter groups ( $i = 1, 2, \dots, N$ )
- $LD$  Large droplet route
- $SR$  Short-range airborne route

51

52 Symbols

53

- $A_0$  Area of source mouth [ $\text{m}^2$ ]
- $AE$  Aspiration efficiency [-]
- $Ar_0$  Archimedes number [-]
- $b_g$  Gaussian half width [m]
- $b_t$  Top-hat half width [m]
- $C_D$  Drag coefficient [-]
- $C_l$  Specific heat of liquid [ $\text{J} \cdot \text{kg}^{-1} \cdot \text{K}^{-1}$ ]
- $C_s$  Specific heat of solid [ $\text{J} \cdot \text{kg}^{-1} \cdot \text{K}^{-1}$ ]
- $C_T$  Correction factor for diffusion coefficient due to temperature dependence [-]
- $d_d$  Droplet diameter [m]
- $d_{d0}$  Droplet initial diameter [m]
- $d_{e1}$  Major axis of eye ellipse [m]
- $d_{e2}$  Minor axis of eye ellipse [m]
- $d_h$  Characteristic diameter of human head [m]
- $d_m$  Mouth diameter [m]
- $d_n$  Nostril diameter [m]
- $D_\infty$  Binary diffusion coefficient far from droplet [ $\text{m}^2 \cdot \text{s}^{-1}$ ]
- $DE$  Deposition efficiency [-]
- $e_{LD}$  Exposure due to large droplet route [ $\mu\text{L}$ ]
- $e_{SR}$  Exposure due to short-range airborne route [ $\mu\text{L}$ ]
- $g$  Gravitational acceleration [ $\text{m} \cdot \text{s}^{-2}$ ]
- $I_v$  Mass current [ $\text{kg} \cdot \text{s}^{-1}$ ]
- $IF$  Inhalation fraction [-]
- $k_c$  Constant ( $=0.3$ ) [-]
- $K_g$  Thermal conductivity of air [ $\text{W} \cdot \text{m}^{-1} \cdot \text{K}^{-1}$ ]
- $LS$  Exposure ratio between large droplet and short-range airborne [-]
- $L_v$  Latent heat of vaporization [ $\text{J} \cdot \text{kg}^{-1}$ ]
- $m_d$  Droplet mass [kg]
- $m_l$  Mass of liquid in a droplet [kg]
- $m_s$  Mass of solid in a droplet [kg]
- $M_0$  Jet initial momentum [ $\text{m}^4 \cdot \text{s}^{-2}$ ]
- $M_w$  Molecular weight of  $\text{H}_2\text{O}$  [ $\text{kg} \cdot \text{mol}^{-1}$ ]
- $MF$  Membrane fraction [-]
- $n$  Number of droplets [n]
- $n_0$  Number of droplets expelled immediately at mouth [n]
- $N_{in}$  Number of droplets entering the inhalation zone [n]
- $N_m$  Number of droplets potentially deposited on mucous membranes [n]
- $N_t$  Total number of released droplets [n]
- $Nu$  Nusselt number [-]
- $p$  Total pressure [Pa]

$p_{v\infty}$	Vapour pressure distant from droplet surface [Pa]
$p_{vs}$	Vapour pressure at droplet surface [Pa]
$Q_{jet}$	Jet flow rate [ $\text{m}^3 \cdot \text{s}^{-1}$ ]
$r$	Radial distance away from jet centreline [m]
$r_d$	Droplet radius [m]
$R$	Radius of jet potential core [m]
$R_g$	Universal gas constant [ $\text{J} \cdot \text{K}^{-1} \cdot \text{mol}^{-1}$ ]
$s$	Jet centreline trajectory length [m]
$S_{in}$	Width of region on sampler enclosed by limiting stream surface [m]
$Sh$	Sherwood number [-]
$St_c$	Stokes number in convergent part of air stream [-]
$St_h$	Stokes number for head [-]
$St_m$	Stokes number for mouth [-]
$t$	Time [s]
$T_0$	Initial temperature of jet [K]
$T_\infty$	Ambient temperature [K]
$T_d$	Droplet temperature [K]
$u_0$	Initial velocity at mouth outlet [ $\text{m} \cdot \text{s}^{-1}$ ]
$u_d$	Droplet velocity [ $\text{m} \cdot \text{s}^{-1}$ ]
$u_g$	Gaussian velocity [ $\text{m} \cdot \text{s}^{-1}$ ]
$u_{gas}$	Gas velocity [ $\text{m} \cdot \text{s}^{-1}$ ]
$u_{gc}$	Gaussian centreline velocity [ $\text{m} \cdot \text{s}^{-1}$ ]
$u_{in}$	Inhalation velocity [ $\text{m} \cdot \text{s}^{-1}$ ]
$u_t$	Top-hat velocity [ $\text{m} \cdot \text{s}^{-1}$ ]
$v_p$	Individual droplet volume considering evaporation [ $\text{m}^3$ ]
$x$	Horizontal distance between source and target [m]
$z$	Jet vertical centreline position [m]
$\rho_0$	Jet initial density [ $\text{kg} \cdot \text{m}^{-3}$ ]
$\rho_\infty$	Ambient air density [ $\text{kg} \cdot \text{m}^{-3}$ ]
$\rho_d$	Droplet density [ $\text{kg} \cdot \text{m}^{-3}$ ]
$\rho_g$	Gas density [ $\text{kg} \cdot \text{m}^{-3}$ ]
$\Delta\rho$	Density difference between jet and ambient air [ $\text{kg} \cdot \text{m}^{-3}$ ]
$\mu_g$	Gas dynamic viscosity [ $\text{Pa} \cdot \text{s}$ ]
$\varphi$	Sampling ratio in axisymmetric flow system [-]
$\alpha_c$	Impaction efficiency in convergent part of air stream [-]

54

## 55 **1. Introduction**

56

57 Despite significant progress in medicine and personal hygiene, seasonal respiratory infections  
58 such as influenza remain a significant threat to human health as a result of more frequent  
59 social contact and rapid genetic evolution of microbes. Disease transmission is a complex and  
60 interdisciplinary process related to microbiology, environmental and social science. The  
61 respiratory activities of an infected person (infected), such as talking and coughing, release  
62 expiratory droplets that contain infectious pathogens, and these expired droplets can be the  
63 medium for transmitting infection. Exposure to these droplets leads to risk of infection and/or  
64 disease. Three possible routes of transmission have been widely recognised and studied: the  
65 airborne, fomite and large droplet (or droplet-borne) routes [1]. The former two are examples  
66 of distant infection, whilst the latter occurs with close contact.

67  
68 When a susceptible individual is in close contact with an infected, the risk of exposure to  
69 exhaled droplets is expected to be at its greatest. The concentration of exhaled droplets is  
70 higher in expired jets than in ambient air. Brankston et al. [2] suggested that transmission of  
71 influenza is most likely to occur at close contact. Close interpersonal contact is ubiquitous in  
72 daily life, such as in offices [3], schools and homes. Although it varies between cultures [4],  
73 the interpersonal distance is normally within 1.5-2 m. Close contact in itself is not a  
74 transmission route, but a facilitating event for droplet transmission. Note that the use of  
75 "droplets" in the remaining text refers to all sizes, down to and including all fine droplets,  
76 such as the sub-micron ones. Two major sub-routes are possible in close contact  
77 transmission. The large droplet sub-route refers to the deposition of large droplets on the  
78 lip/eye/nosril mucosa of another person at close proximity, resulting in his or her self-  
79 inoculation. Dry surroundings enable the exhaled droplets to evaporate, and some rapidly  
80 shrink to droplet nuclei. The fine droplets and droplet nuclei can also be directly inhaled,  
81 which is the short-range airborne sub-route. Both sub-routes involve direct exposure to the  
82 expired jet, which is affected by the interacting exhalation/inhalation flows of the two  
83 persons. For example, head movement can change the orientation of the expired flow, and the  
84 mode of breathing affects the interaction. The significance of breathing mode (mouth/nose)  
85 and distance between people in cross-infection risk has been widely studied [5]. Body  
86 thermal plumes can also interact with the expired jet from the infected and with potential  
87 inhalation of the flow by the susceptible person [1].

88  
89 *It remains an open question whether either of the two sub-routes is dominant, or both are*  
90 *important.* The large droplet route has been believed to be dominant for most respiratory  
91 infections [2] since Flügge [6] and Chapin [7]. Some epidemiological studies have even  
92 assumed respiratory infections to be due to large droplets whenever close contact  
93 transmission is observed [8]. Liu et al. [9] showed that both the large droplet route and the  
94 short-range airborne route can be important within 1.5 m. However, their computational fluid  
95 dynamics (CFD) modelling considered only a very small number of droplets, and the  
96 frequency of droplet deposition on the mucosa was not estimated. Except for that study by  
97 Liu et al. [9], comparison of the two sub-routes has rarely been reported. In the general  
98 discipline of exposure science, particle inhalability has been studied in depth, due to the  
99 potential health impact of particles when inhaled; see Vincent [10] for a comprehensive  
100 review. There are also considerable data on particle inhalability in humans. However, the  
101 short-range airborne route, or expired droplet inhalability at close contact, that we consider  
102 here differs from conventional particle inhalability (e.g., [11]) in at least two aspects. First, it  
103 is not the room air flow that affects inhalability, but the expired air stream from the source  
104 person. The inhalability depends upon whether the susceptible person's mouth or nose is  
105 located within or partially within the cone of the expired jet from the source person. The size  
106 of the expired droplets changes due to evaporation after being exhaled and before being  
107 inhaled or deposited on the mucous membranes. Large droplet deposition on mucous  
108 membranes has rarely been studied in combination with their inhalation. Kim et al. [12]  
109 investigated aerosol-based drug delivery for a 7-month infant, taking both large droplet and  
110 short-range routes into account using CFD. They found that droplet deposition was  
111 determined more by head direction than by inhalation, suggesting the importance of close  
112 contact parameters.

113  
114 The importance of identifying the dominant/important sub-route(s) in close contact is  
115 obvious. There are significant implications for the choice and development of effective  
116 intervention measures. If the short-range airborne sub-route is dominant, a face mask (a

117 typical droplet precaution) will not be sufficient because these masks cannot remove fine  
118 droplets. This study aims to tackle the question of the relative importance of the two exposure  
119 sub-routes using simple analysis.

120

## 121 **2. Methods**

122

123 A mathematical model is developed here, based on the simple dynamics of expired jets. As in  
124 inhalability studies, we consider the droplet inhalation and deposition processes as particle  
125 sampling (e.g. [13]).

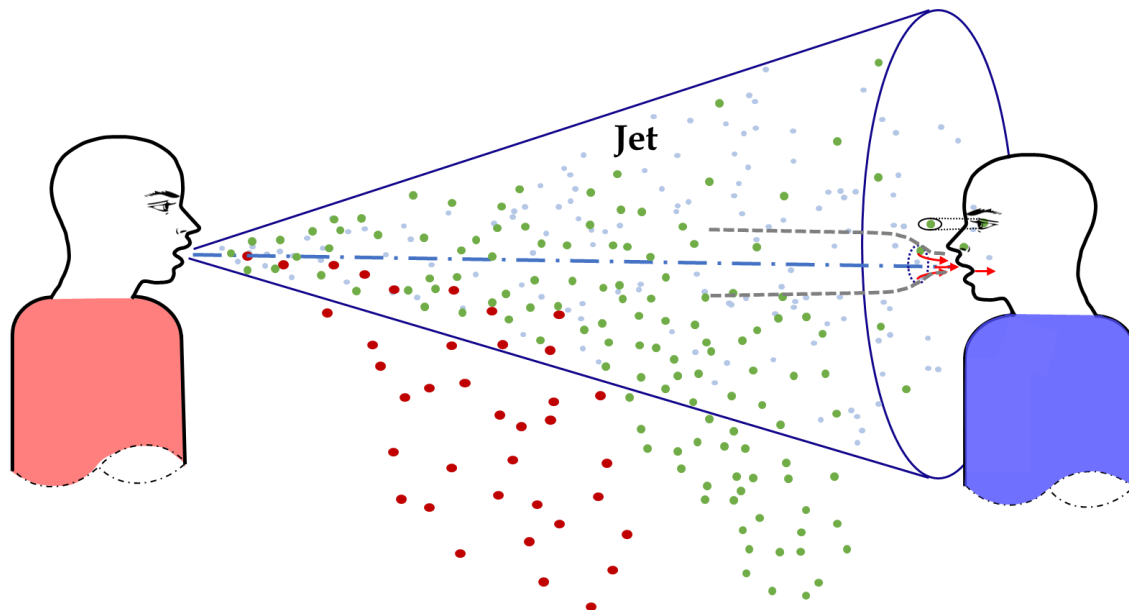
126

127 The large droplet route and short-range airborne route are illustrated in [Figure 1](#) for two  
128 standing persons, who might be in conversation or simply in face-to-face contact, within less  
129 than 2 m. One individual is identified as the source (the infected) and the other as the target  
130 (the susceptible person). Droplets can be directly deposited on the susceptible person's facial  
131 membranes (eyes, nostrils and mouth; i.e., the large droplet sub-route), whilst those inhaled  
132 via oral breathing are categorised into the short-range airborne sub-route. The terminologies  
133 "large droplet" and "short-range airborne" here apply to an overall droplet size range, and  
134 each size of droplets (as shown in [Figure 2](#)) will have opportunities to be deposited or  
135 inhaled, regardless of its diameter. Note that these two sub-routes are considered as two  
136 separate processes; that is, the large droplet and short-range airborne routes do not happen  
137 simultaneously, and infection occurs through the mouth in both cases. The environmental  
138 conditions include air temperature (25°C), relative humidity (RH = 50%) and atmospheric  
139 pressure (101,325 Pa). The room air flows are also not considered (i.e., background air at 0  
140 m/s). Droplets were released from a height of 1.75 m, considering that both individuals were  
141 standing.

142

143 The exposure is defined as the total volume of droplets to which the susceptible person is  
144 exposed, in units of  $\mu\text{L}$ . The riskiest situation was investigated here, that in which the  
145 susceptible person is in *direct* face-to-face contact with the source. For the short-range  
146 airborne route, we assumed that the target took a breath exactly when the droplet-laden air  
147 flow exhaled by the infected reached him or her; for the large droplet route, the susceptible  
148 person was assumed to hold his or her breath with the mouth open. The two mouths are at the  
149 same height; see [Figure 1](#). Hence, we studied perhaps the worst scenario in terms of large  
150 droplet transmission. Our model considers the spread of the exhalation jet, and the dispersion  
151 and evaporation of expired droplets, as an example of aerosol sampling, a process analogous  
152 to inhalation and consistent with human facial features. We used Matlab for implementing the  
153 prediction. The used models in terms of airflow and particle deposition have been previously  
154 validated.

155



156  
157 **Figure 1.** Schematic diagram of close contact scenario with exhalation from the infected  
158 (left) and inhalation through the mouth of the susceptible person (right).  
159

160 *2.1 Exposure calculation*

161 The exposure via the large droplet and short-range airborne sub-routes at any horizontal  
162 distance  $x$  can be calculated as:

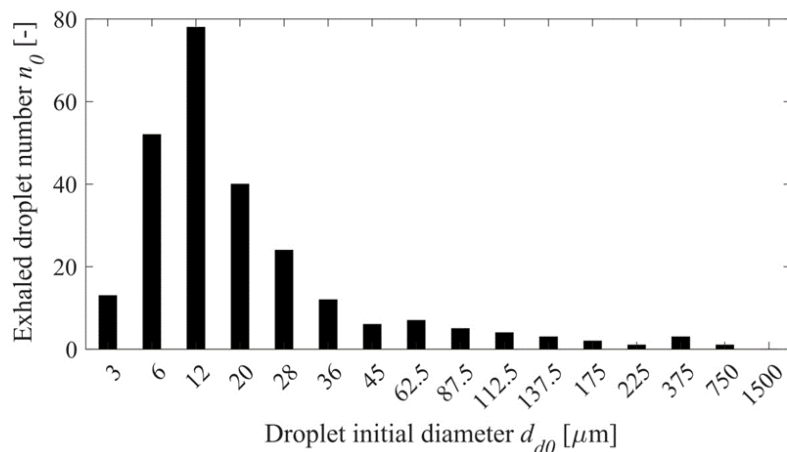
163  
164 
$$e_{LD}(x) = \sum_{i=1}^N n_{0i} \cdot v_{pi} \cdot MF_i \cdot DE_i \tag{1}$$

165 
$$e_{SR}(x) = \sum_{i=1}^N n_{0i} \cdot v_{pi} \cdot IF_i \cdot AE_i \tag{2}$$

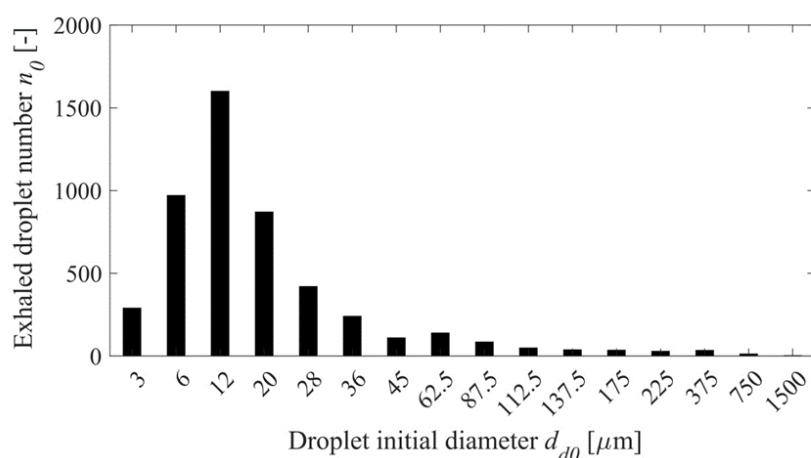
166  
167 where subscript *LD* and *SR* denote the large droplet route and short-range airborne route,  
168 respectively;  $i$  stands for droplets sorted into groups based on diameter ( $i = 1, 2, \dots, N$ );  $n_0$  is  
169 the number of droplets expelled from the source mouth at the moment of exhalation;  $v_p$  is  
170 the individual droplet volume, taking into account evaporation; *MF* is the membrane fraction;  
171 *DE* is the deposition efficiency; *IF* is the inhalation fraction; and *AE* is the aspiration  
172 efficiency. These variables will be defined more specifically in the following sections. Our  
173 adopted index *IF* is not to be confused with intake fraction as used for example in Berlanga et  
174 al. [14]. The droplet number generated in expiratory activities has been measured by many  
175 researchers, e.g. [15-16]. To encompass a wide size range, the classical experimental dataset  
176 by Duguid [17] was adopted. The number distributions of different-sized droplets, as  
177 generated by two different exhalatory processes – counting out loud from ‘1’ to ‘100’ once  
178 (i.e., talking), and coughing once [17] – are shown in Figure 2 and refer to the  $n_0$  values.  
179 The total volumes of droplets released by talking and coughing are 0.32  $\mu\text{L}$  and 7.55  $\mu\text{L}$   
180 respectively, which are calculated as the sum of droplet volume of each size. The diameters  
181 of the expired droplets may extend down to the submicron scale; however, we do not have  
182 access to a full and consistent set of data that include these submicron sizes.  
183

184 To compare the relative contribution of the two sub-routes, an *LS* exposure ratio is defined at  
185 each horizontal distance  $x$ . If the *LS* ratio is greater than 1, the large droplet route dominates,  
186 and vice versa.

187  
188 
$$LS(x) = e_{LD}(x)/e_{SR}(x) \tag{3}$$
  
189



(a)



(b)

190 **Figure 2.** Number distributions of exhaled droplets at the point of mouth opening. (a) Talking  
191 (counting from ‘1’ to ‘100’ once) [n]; (b) Coughing once [n].

192

### 193 2.2 Velocity profiles in the expired jet

194 As a first approximation, the exhaled air flow from the infected source may be treated as a  
195 turbulent round jet, including a flow establishment zone and an established flow zone. The  
196 velocity profiles and the flow rate can be obtained by various jet theories. Given the fact that  
197 human exhalation can be complicated in terms of airflow fluctuations, individual differences,  
198 and exhaled flow directions [18], here we chose the classic jet formulas in Lee and Chu [19].  
199 Let  $s$  be the centreline distance travelled by the jet and  $d_m$  the source mouth diameter (i.e.  
200 the jet opening, assumed to be 2 cm [20]). The maximum length of the flow establishment  
201 zone is  $6.2d_m$ .

202

203 In the flow establishment zone ( $s \leq 6.2d_m$ , Gaussian profile),

204

$$205 \quad u_g = u_0; r \leq R \quad (4)$$

$$206 \quad u_g = u_0 \exp\left[-\frac{(r-R)^2}{b_g^2}\right]; r \geq R \quad (5)$$

$$207 \quad Q_{jet} = \pi b_g^2 u_0 \quad (6)$$

$$208 \quad b_g = 0.5d_m + 0.033355s \quad (7)$$

209

210 In the established flow zone ( $s > 6.2d_m$ , Gaussian profile),

211  
212  $u_{gc} = 6.2u_0(d_m/s)$  (8)

213  $Q_{jet} = 0.286 \cdot M_0^{\frac{1}{2}} \cdot s = \pi b_g^2 u_{gc}$  (9)

214  $b_g = 0.114s$  (10)

215  
216 where  $u_g$  is the Gaussian velocity;  $u_0$  is the initial velocity at the source mouth outlet;  $r$  is  
217 the radial distance away from the jet centreline;  $R$  is the radius of the jet's potential core;  $b_g$   
218 is the Gaussian half width;  $Q_{jet}$  is the jet flow rate;  $u_{gc}$  is the Gaussian centreline velocity;  
219 and  $M_0 = \frac{\pi}{4} d_m^2 u_0^2$  is the initial momentum. The velocities in the jet cone are used to  
220 calculate the trajectories of the expired droplets.

221  
222 We also take the average velocity on a cross-section plane, which gives a top-hat profile. The  
223 average velocities are used to calculate the particle deposition.

224  
225 In the flow establishment zone ( $s \leq 6.2d_m$ , top-hat profile),  
226  $u_t = \frac{d_m u_0}{2b_t}$  (11)

227  $b_t = 0.5d_m + 0.079355s$  (12)

228  
229 In the established flow zone ( $s > 6.2d_m$ , top-hat profile),  
230  $u_t = u_{gc}/2$  (13)

231  $b_t = \sqrt{2}b_g = 0.16s$  (14)

232  
233 where  $u_t$  is the top-hat velocity;  $b_t$  is the top-hat half width.

234  
235 We use the measured velocity of particles exhaled by different respiratory activities at the  
236 moment of mouth opening as reported by Chao et al. [21]. The average velocity at the mouth  
237 is 3.9 m/s for speaking and 11.7 m/s for coughing.

238  
239 Under isothermal conditions, the jet centreline is assumed to be straight. The exhaled air  
240 temperature (assumed to be 35.1°C, averaged between patients with asthma and control  
241 subjects [22]) generally differs from the environmental temperature (typical room  
242 temperature 25°C). In this case, the jet trajectory would curve upwards [23] as in the  
243 following equations:

244  
245  $\frac{z}{\sqrt{A_0}} = 0.0354 Ar_0 \left( \frac{x}{\sqrt{A_0}} \right)^3 \sqrt{\frac{T_0}{T_\infty}}$  (15)

246  $Ar_0 = \frac{g\sqrt{A_0} \Delta\rho}{u_0^2 \rho_0}$  (16)

247  
248 where  $z$  is the vertical centreline position;  $A_0 = \pi d_m^2 / 4$  is the area of the source mouth;  
249  $Ar_0$  is the Archimedes number;  $T_0$  is the initial temperature of the jet;  $T_\infty$  is the ambient  
250 temperature;  $g$  is the gravitational acceleration;  $\rho_0$  is the jet initial density;  $\Delta\rho = \rho_\infty - \rho_0$   
251 is the density difference between the jet and ambient air. Note that  $x$  is the horizontal distance  
252 between the source and the target, whilst  $s$  is the jet centreline trajectory length. Each  $x$   
253 corresponds to an  $s$  value, and  $s$  is slightly larger than  $x$ .

254  
255 *2.3 Droplet evaporation and dispersion*



256 To ensure a significant number of droplets depositing on face/membranes or entering the  
 257 inhalation zone in calculating  $MF$  and  $IF$  (especially for droplets with large sizes), a total of  
 258 5000 droplets greater than  $50\ \mu\text{m}$  and 1600 droplets smaller than  $50\ \mu\text{m}$  were released. The  
 259 simulation of droplet motion and evaporation was based on an existing model developed and  
 260 validated in Wei and Li [20]. The governing equations for motion, mass flux and heat transfer  
 261 are listed below. Droplets were modelled to be released randomly from the source mouth,  
 262 which was divided into 1600 segments. The maximum distance studied is 2 m. Our prediction  
 263 of droplet dispersion starts from the release at the source mouth and ends when falling on the  
 264 ground or reaching 2 m. At each 0.1 m, data such as droplet velocity, position and size  
 265 change were recorded.

$$268 \frac{d\mathbf{u}_d}{dt} = \frac{3\rho_g C_D}{4d_d \rho_d} (\mathbf{u}_{gas} - \mathbf{u}_d) |\mathbf{u}_{gas} - \mathbf{u}_d| + \mathbf{g} \quad (17)$$

$$270 \frac{dm_d}{dt} = -I_v = \frac{2\pi p d_d M_w D_{\infty} C_T S h}{R_g T_{\infty}} \ln \left( \frac{p - p_{vs}}{p - p_{v\infty}} \right) \quad (18)$$

$$272 (m_l C_l + m_s C_s) \frac{dT_d}{dt} = \pi d_d^2 K_g \frac{T_{\infty} - T_d}{r_d} Nu - L_v I_v \quad (19)$$

#### 274 2.4 Deposition

275 The droplet membrane fraction ( $MF$ ) is defined as the ratio of the number of droplets that  
 276 are potentially deposited on the mucous membranes,  $N_m$ , to the total number of released  
 277 droplets,  $N_t$ .

$$279 MF = \frac{N_m}{N_t} \quad (20)$$

281 The process of deposition due to the large droplet route is illustrated in Figure 3b. The total  
 282 surface area of the two eyes is  $6\ \text{cm}^2$  and that of the two nostrils is  $2\ \text{cm}^2$  [24]. The mouth is  
 283 approximated as a circle with a diameter of 2 cm [20]. The total surface area of the eyes,  
 284 nostrils and lips is approximately only  $15\ \text{cm}^2$  [25], compared with the average area for a  
 285 head of  $1300\ \text{cm}^2$  [26]. A diagram of extracted facial features is shown in Figure 3a, with the  
 286 eyes being treated as ellipses, the nose and mouth being circles. The vertical distance between  
 287 the eyes and nose is 3.07 cm, and the distance between the eyes and mouth is 5.64 cm [27].  
 288 The number of droplets that are potentially deposited on the mucous membranes,  $N_m$ , can be  
 289 obtained by deciding whether a particular droplet is within the projected cylindrical volumes  
 290 just in front of the eye ellipses or nose/mouth circles (see Figure 3b). Only a fraction of these  
 291 droplets will deposit, while others would follow the airflow trajectory around the face. This  
 292 enables the dispersion of droplets in the exhaled jet to be fully considered before arriving at  
 293 the head of the susceptible person. This simple model does not consider the opening and  
 294 closing of the eyes and mouth or that the nostril openings may not always be facing forward.  
 295 By assuming that the eyes and mouth are always open and that droplets can always be  
 296 directly deposited onto the nostrils, the model may overestimate the rate of large droplet  
 297 deposition.

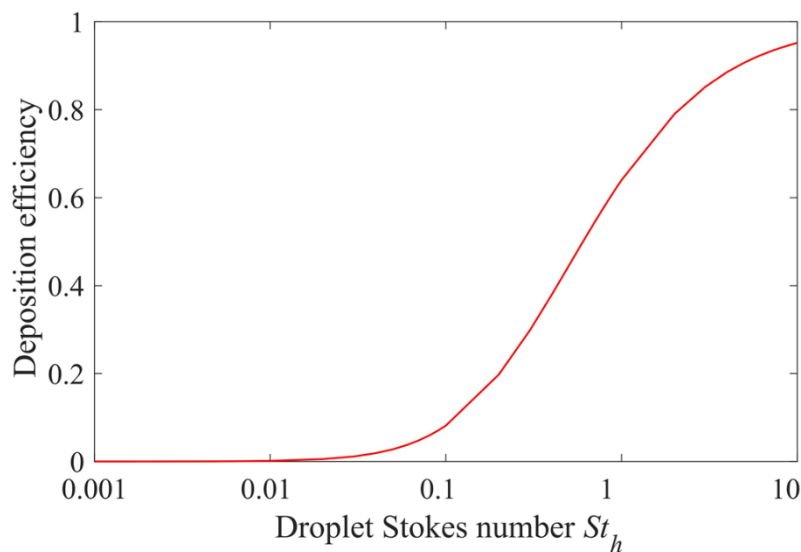
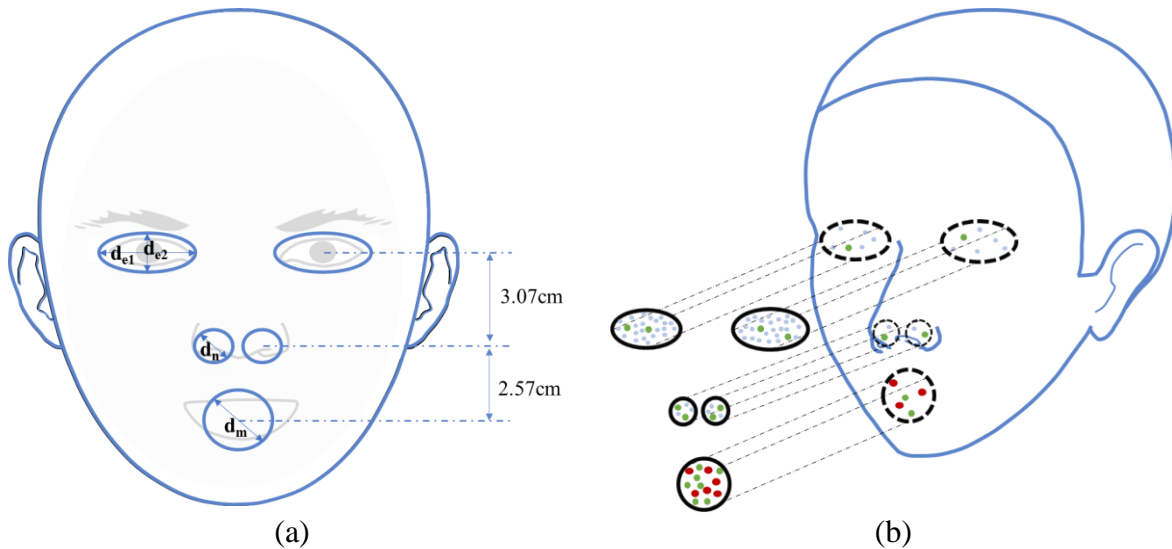
299 The deposition efficiency ( $DE$ ) represents the probability of deposition, which is a function  
 300 of the droplet Stokes number, a dimensionless number characterising the behaviour of  
 301 droplets suspended in a fluid flow. Droplets with a small Stokes number follow the  
 302 surrounding fluid flow, whilst those with a large Stokes number tend to continue their

303 trajectory under inertia and are deposited. We approximate the head as a sphere. The droplet  
 304 deposition efficiency on a sphere was first considered by Langmuir and Blodgett [28] (see  
 305 Figure 3c). The model given by Equation (21) was in reasonable agreement with the  
 306 experimental data of Walton and Woolcock [29]. The theory was further confirmed by  
 307 measurement by Hähner et al. [30] and Waldenmaier [31]. The horizontal location  
 308 differences among eyes, nostrils and mouth on the sphere were neglected. They were  
 309 assumed to be on the same plane, although a spherical model was used in calculating the  
 310 deposition.

$$312 \quad DE = \frac{St_h^2}{(St_h + 0.25)^2} \quad (21)$$

$$313 \quad St_h = \frac{u_t}{d_h/2} \frac{\rho_d d_d^2}{18\mu_g} \quad (22)$$

314 where  $St_h$  is the Stokes number for an approximate spherical head;  $\rho_d$  is the droplet  
 315 density;  $d_d$  is the droplet diameter;  $d_h = 0.2 \text{ m}$  is the characteristic diameter of the human  
 316 head;  $\mu_g$  is the gas dynamic viscosity. Considering the distributions of facial organs in the  
 317 expired jet,  $u_t$  was used for Stokes number calculation.  
 318  
 319



(c)

320  
321 **Figure 3.** (a) Extraction of human facial features and their dimensions in our model ( $d_{e1} =$   
322  $2.76$  cm,  $d_{e2} = 1.38$  cm,  $d_n = 1.13$  cm,  $d_m = 2.00$  cm); (b) illustration of the large droplet route,  
323 where only droplets deposited on mucous membranes are considered to result in exposure;  
324 note that only a fraction of droplets entering cylindrical volumes would eventually deposit;  
325 (c) variation of capture efficiency on a sphere with the Stokes number [28-31].

### 326 327 2.5 Inhalation

328 The inhalation process is treated as an anisokinetic sampling process, with the human head  
329 approximated as a spherical aerosol sampler and the target mouth as a sampling orifice. There  
330 have been many efforts since the 1970s to predict aspiration efficiency ( $AE$ , ratio of inhaled  
331 concentration to mainstream concentration, also referred to as inhalability), such as those of  
332 Ogden and Birkett [32], Armbruster and Breuer [33] and Vincent and Mark [34]. Many  
333 aspects of  $AE$  have been studied, using manikin experiments [35-38], theoretical models [13,  
334 39] and CFD simulations [11, 40]. Great discrepancy exists among empirical equations. For  
335 example, the International Standards Organization (ISO) convention assumes a continuous  
336 decline of inhalability with the increase of aerosol diameter, while according to the American  
337 Conference of Governmental Industrial Hygienists (ACGIH) the aspiration efficiency levels  
338 off at approximately 0.5 [36]. Many equations were derived under specific experimental  
339 settings, thus failing to consider every potential factor. Note that the largest droplet diameters  
340 considered in the above-mentioned studies were  $185 \mu\text{m}$ , which is close to the large droplet  
341 range as defined here. Although exhaled droplets can be as large as  $1 \text{ mm}$ , such sizes are rare,  
342 and these droplets are probably not as infectiously important as finer droplets, which contain  
343 most of the viruses.

344  
345 The combined effect of mainstream air flow and sampling inhalation is that the streamlines  
346 first diverge when approaching the sampler, and then converge into the orifice. Dunnett and  
347 Ingham [41] established a 3D inhalation model with a spherical blunt sampler, which was  
348 shown in satisfactory agreement with the experimental results by Ogden and Birkett [32], as  
349 shown in Figure 4a. In contrast to the other models mentioned above, a complete set of  
350 influential factors was considered, without restrictions on the velocity and droplet size, thus  
351 providing important theoretical insights. Therefore, this inhalation model was adopted here.

$$352 \quad \varphi = \frac{d_m^2 u_{in}}{d_h^2 u_{gc}} \quad (23)$$

$$353 \quad S_{in} = d_h (\varphi/3)^{1/3} \quad (24)$$

354  
355 where  $\varphi$  is the sampling ratio for the axisymmetric flow system;  $u_{in}$  is the inhalation  
356 velocity ( $1 \text{ m/s}$ );  $S_{in}$  is the width of the region on the sampler enclosed by the limiting  
357 stream surface. Note that we only consider the specific situation in which the negative mouth  
358 normal direction and the air flow direction are identical.

359  
360  
361  $IF$  is simply the proportion of droplets that can enter the inhalation zone enclosed by the  
362 limiting streamlines (Figure 4b).

$$363 \quad IF = \frac{N_{in}}{N_t} \quad (25)$$

364  
365 where  $N_{in}$  is the number of droplets entering the inhalation zone;  $N_t$  is the total number of  
366 released droplets at the mouth of the infected.

368  
 369 The inhalation zone is taken as a circular region in front of the target mouth with a diameter  
 370  $S_{in}$  as calculated by the aspiration efficiency model (Equation (24)). We can obtain  $N_{in}$  by  
 371 determining whether a particular droplet is within the inhalation zone. The position of the  
 372 inhalation zone is also where the divergent centrelines become convergent (plane  $PP'$  in  
 373 Figure 4a). We ignore the small gap between the susceptible person's mouth and the  $PP'$   
 374 plane. A fraction of these  $N_{in}$  droplets will deposit on the target surface, while the others  
 375 will be inhaled.

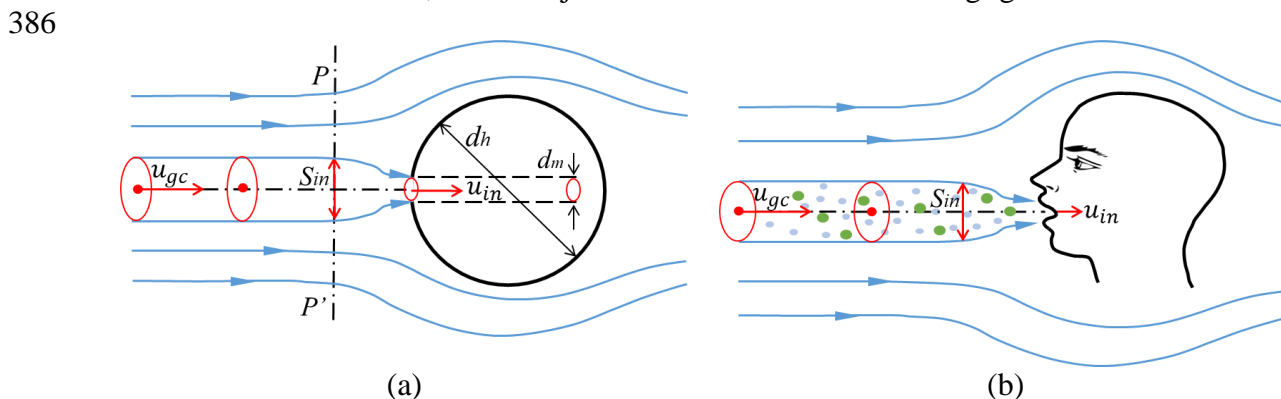
$$377 \quad St_m = \frac{u_{gc} \rho_d d_d^2}{d_m 18\mu_g} \quad (26)$$

$$378 \quad St_c = \frac{St_m d_h^2 \varphi}{d_m^2} \quad (27)$$

$$379 \quad \alpha_c = 1 - \frac{1}{1+k_c St_c} \quad (28)$$

$$380 \quad AE = 1 + \alpha_c \left( \frac{d_m^2}{S_{in}^2} - 1 \right) \quad (29)$$

381  
 382 where  $St_m$  is the Stokes number for the mouth;  $St_c$  the Stokes number in the convergent part;  
 383  $\alpha_c$  the impaction efficiency in the convergent part; and the constant  $k_c$  equals 0.3 when  
 384 directly facing the incoming flow. Note that  $u_{gc}$  was adopted as the oncoming flow velocity  
 385 for inhalation calculation, since the jet curvature within 2 m was negligible.



387 **Figure 4.** (a) Schematic diagram of aerosol sampling process with a spherical blunt sampler;  
 388 (b) Illustration of the short-range airborne route with mouth inhalation. Note that only a  
 389 fraction of the droplets entering the inhalation zone would eventually be inhaled.

### 391 3. Results

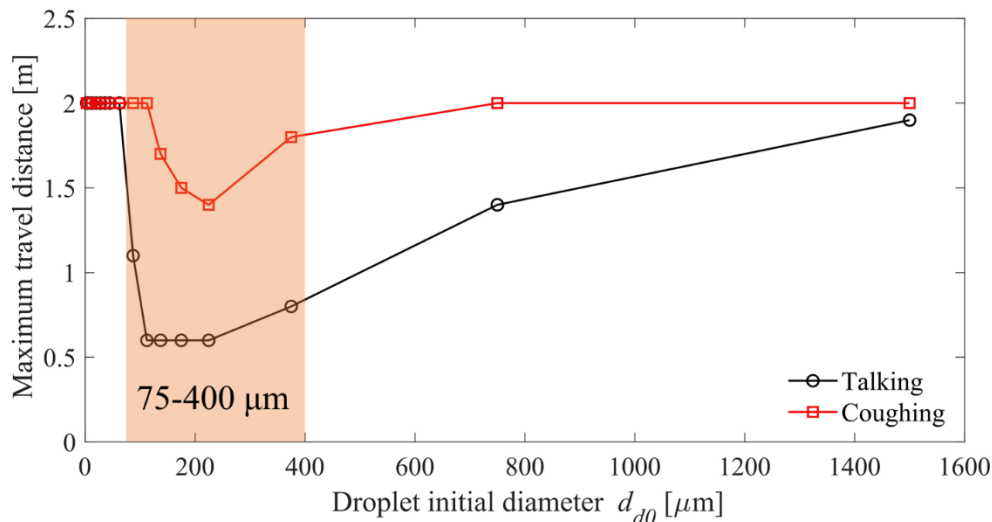
#### 393 3.1 Medium size droplets (75 to 400 $\mu\text{m}$ ) travel the shortest distance

394 Figure 5a shows the maximum travel distance for various droplet sizes. Note that the  
 395 travel distance here was defined as the longest distance at which droplets could be  
 396 detected, so the maximum value is perforce 2 m in this study, which does not necessarily  
 397 mean that these droplets could not travel further. The shortest distance was travelled by  
 398 droplets with diameters of approximately 112.5 to 225  $\mu\text{m}$  for talking and 175 to 225  $\mu\text{m}$   
 399 for coughing. In general, within the close range (2 m) studied, the small size group (<75  
 400  $\mu\text{m}$ ) would follow the air stream, being widely dispersed. The medium size group (75 to  
 401 400  $\mu\text{m}$ ) would be dominated by gravity, falling rapidly to the ground. The very large  
 402 size group (>400  $\mu\text{m}$ ) would be dominated by inertia and travel a longer distance. The  
 403 trend of our results is consistent with the CFD results by Zhu et al. [42] and Sun and Ji  
 404 [43], although they did not quantify it. In the above discussion of travel distance, we

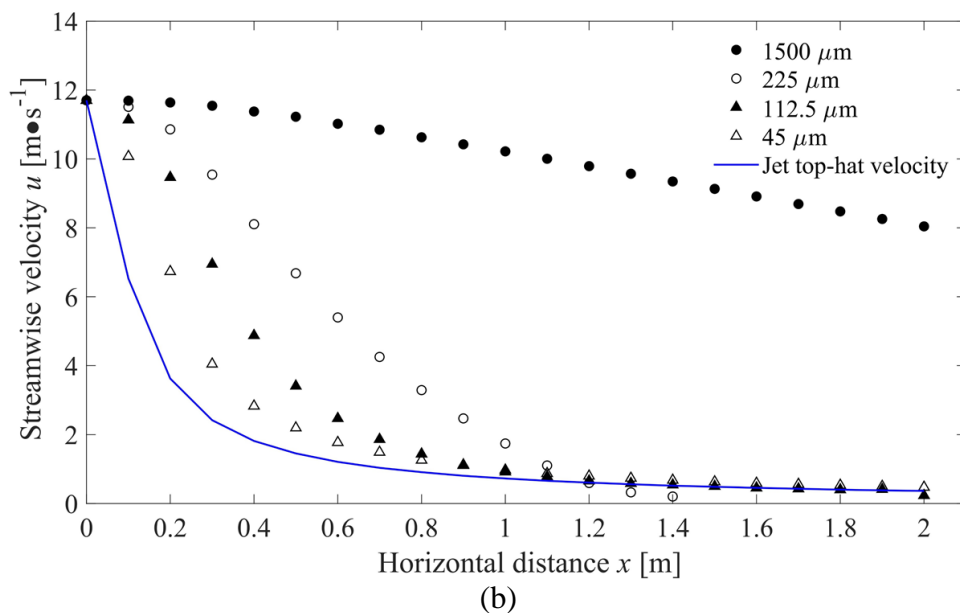
405 noted the effect of size groups to avoid confusion with the relationship between droplet  
 406 size and *exposure* in later discussion.

407

408 To elucidate the above results, the calculated velocities of air and droplets in a cough jet  
 409 are compared for four droplet sizes: 1500, 225, 112.5 and 45  $\mu\text{m}$  (Figure 5b). The smaller  
 410 droplets (45  $\mu\text{m}$ ) have a very rapid momentum-response time (Table 1), which allows  
 411 them to quickly follow the exhaled air stream, whilst the larger droplets (1500  $\mu\text{m}$ )  
 412 maintain their own velocity due to their more sluggish momentum-response time. This  
 413 suggests that over a short distance, very large droplets are unlikely to settle.



The maximum distance considered is 2 m and droplets could travel further  
 (a)



414 **Figure 5.** (a) Predicted maximum travel distances for various sizes of droplets during talking  
 415 and coughing activities. Note that we consider a maximum travel distance of 2 m. (b)  
 416 Differences between the averaged streamwise velocity of droplets with diameters of 1500,  
 417 225, 112.5 and 45  $\mu\text{m}$  after being released, and the jet velocity based on top-hat profile at  
 418 various distances from the mouth of the infected during coughing.  
 419

420

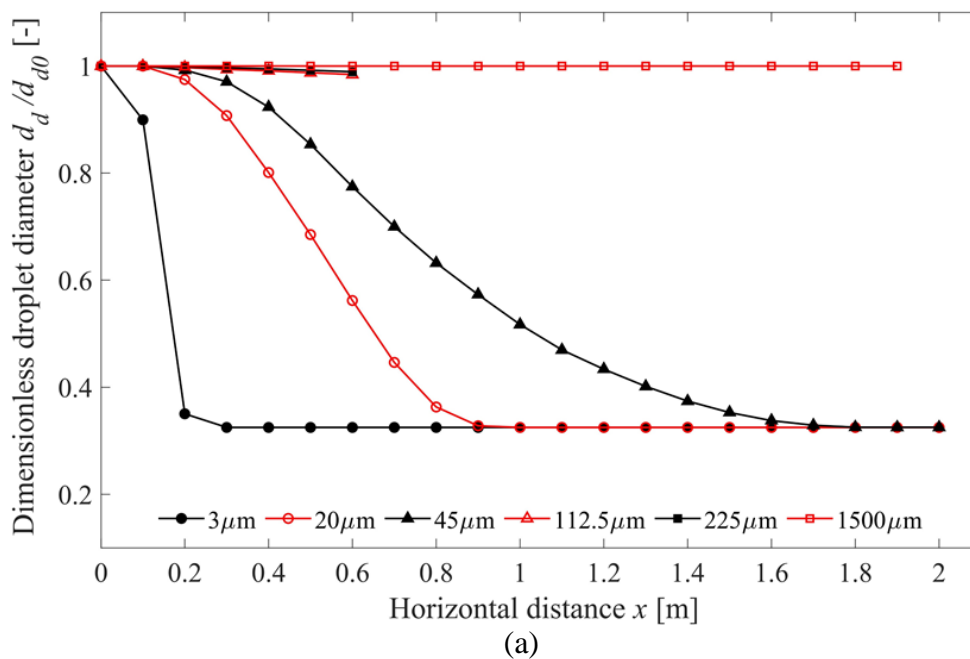
421 **Table 1.** Droplet dynamics comparison in a cough jet.  
422

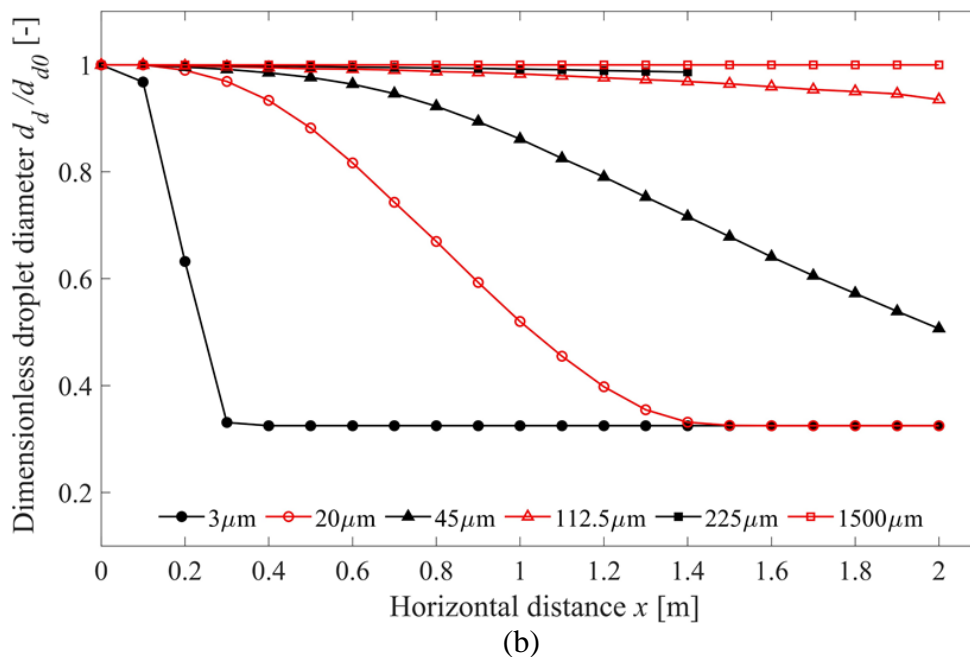
Diameter ( $\mu\text{m}$ )	Relaxation time (s)	Settling velocity (m/s)	Reynolds number at the mouth exit (-)	Stopping distance (m)
1500	6.72E+00	6.59E+01	1.16E+03	8.83E+00
225	1.51E-01	1.48E+00	1.73E+02	5.04E-01
112.5	3.78E-02	3.71E-01	8.67E+01	1.67E-01
45	6.05E-03	5.93E-02	3.47E+01	3.64E-02

423

424 *3.2 Significant impact of exhalation velocity on travel distance and size change*

425 Evaporation and falling processes compete after droplets are expelled from the mouth, so a  
426 critical size exists at which the falling time equals the evaporation time [44]. Various ambient  
427 environments (i.e., RH, temperature, etc.) and initial injection velocities also influence the  
428 droplet thermodynamics [45]. In these two studies by Wells [44] and Xie et al. [45], droplets  
429 were assumed to be perfect spheres that evaporated to a final diameter because of the  
430 existence of insoluble solids [20]. The change in dimensionless droplet diameter was  
431 compared for several typical initial sizes covering the whole range studied (see Figure 6).  
432 Because it was assumed that all droplets shared the same initial solid volume ratio, the final  
433 dimensionless diameter value remained constant for each size. For the assumed droplet  
434 composition here, the final size is 32.5% of the original diameter. Exhalation velocity was  
435 shown to have a significant impact on droplet travel distance for the medium size group (75  
436 to 400  $\mu\text{m}$ ). The droplets of 112.5  $\mu\text{m}$  and 225  $\mu\text{m}$  in diameter travelled more than twice as  
437 far due to coughing than due to talking. Although the medium and very large droplets  
438 continued to shrink throughout their 2-m flight, the small droplets evaporated much more  
439 quickly, reaching their final size at some distance short of 2 m. The 3- $\mu\text{m}$  droplets shrank  
440 rapidly within the first 0.1 m.

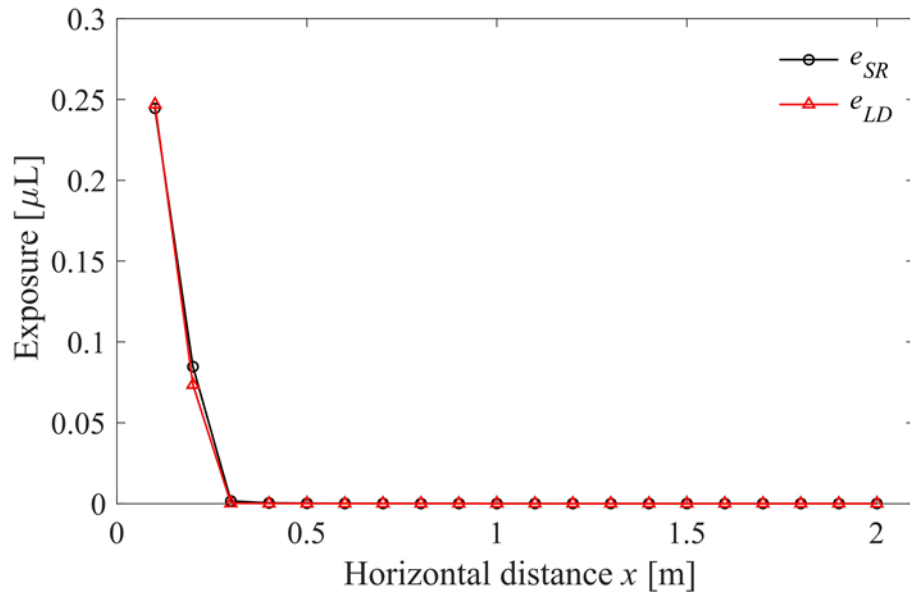




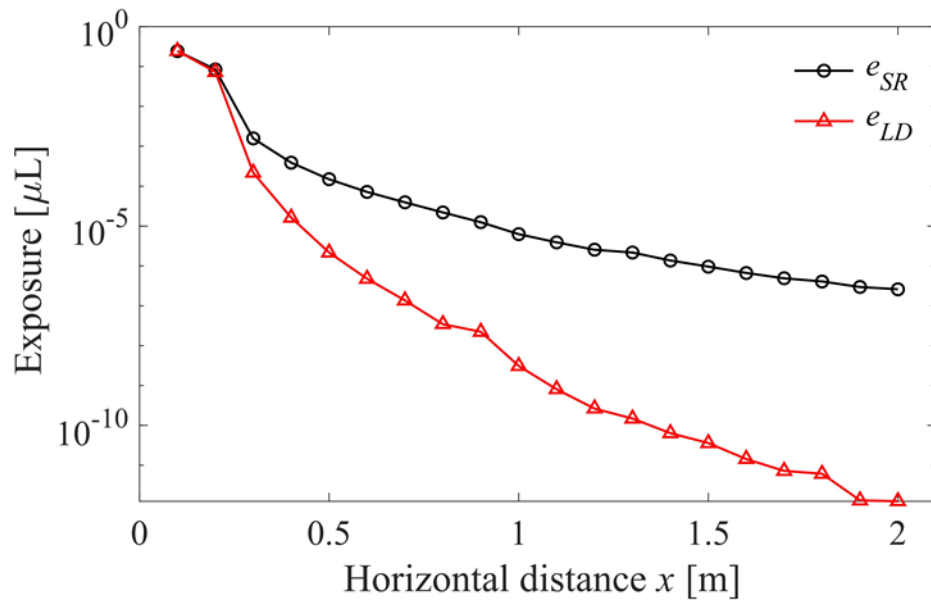
441 **Figure 6.** Changes in dimensionless droplet diameter while travelling away from the mouth  
 442 of the infected for (a) talking; (b) coughing. Note that once all simulated droplets of a  
 443 particular size land on the ground, no size is shown.  
 444

### 445 3.3 Total exposure

446 The total exposure of the susceptible person is shown in [Figure 7](#) as a function of distance  
 447 from the infected. To facilitate comparison, the exposure profile drawn on a logarithmic scale  
 448 is also included. As expected, the exposure generally decreases as distance increases for both  
 449 the large droplet and short-range airborne sub-routes. As shown in [Figure B4\(a\)](#), the  
 450 coughing inhalation zone is smaller than target mouth at 0.1-0.3 m. It is too soon for droplets  
 451 to disperse widely within 0.3 m, so more of them would be encompassed into the inhalation  
 452 zone with an increase of size. The short-range inhalation exposure increases from 0.1-0.3 m  
 453 is due to the enlargement of inhalation zone area, which directly influences the inhalation  
 454 fraction ( $IF$ ). From 0.3 m on, the overall decrease of exposure is dominated by jet dilution.  
 455 As a whole, the exposure due to talking is an order of magnitude lower than that due to  
 456 coughing for the situation considered here. The talking exposure was estimated based on  
 457 prolonged loud speaking in which subjects were asked to count from ‘1’ to ‘100’, whilst  
 458 coughing exposure was based on a single cough with the mouth initially closed. Given the  
 459 same time period as for talking, coughing still causes a higher infection risk than talking  
 460 considering coughing frequency of patients [46]. The total exposure value decreased by  
 461 several orders of magnitude to almost zero at 0.3 m for talking and 0.8 m for coughing. A  
 462 steep decline could also be detected in the logarithmic plots at the same distance. Notably,  
 463 and unexpectedly, the short-range airborne route posed a greater exposure risk than the large  
 464 droplet route, for both respiratory activities, at most distances in this close-range study,  
 465 especially the longer distances.

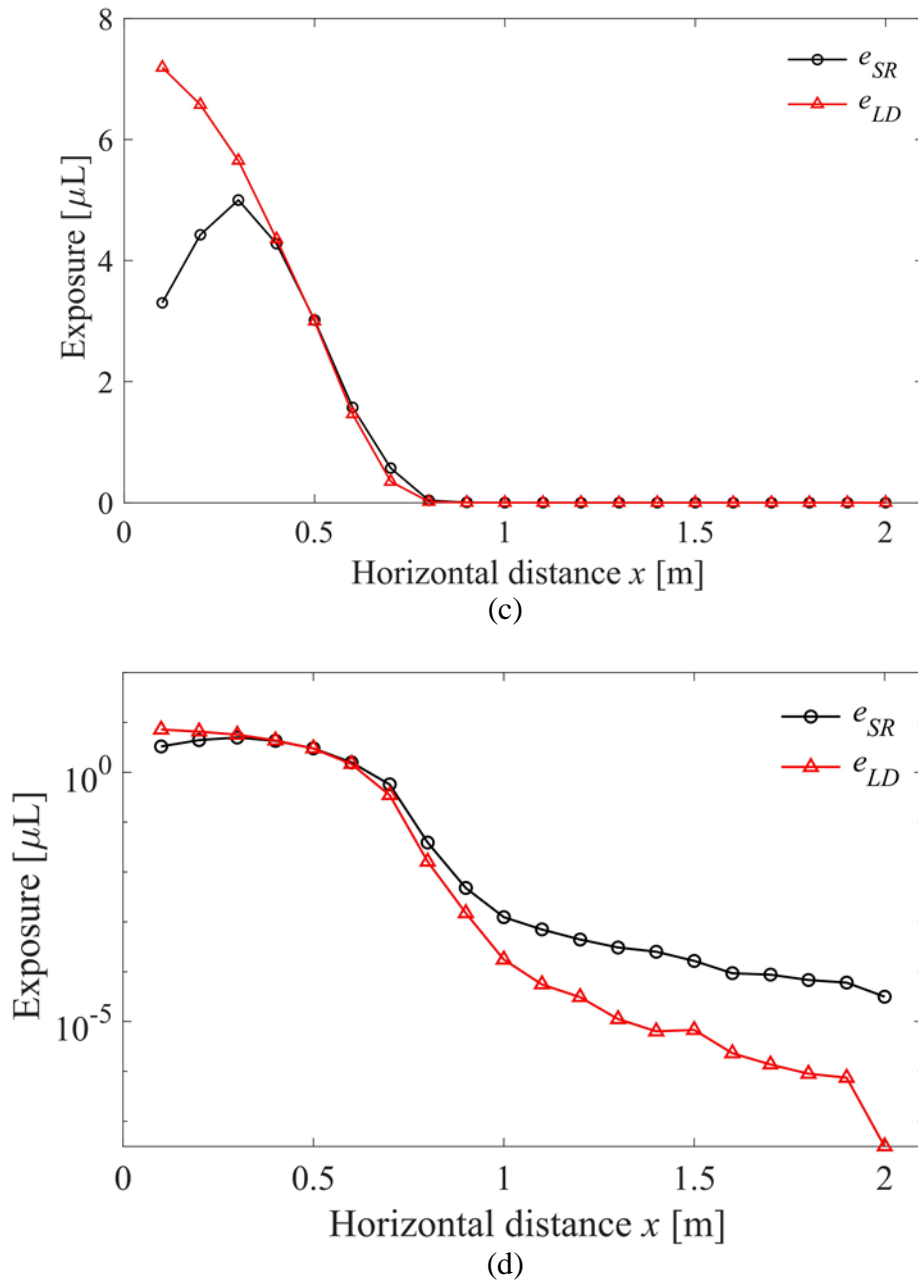


(a)



(b)





466  
 467 **Figure 7.** Total exposure for (a) talking (i.e. prolonged counting from ‘1’ to ‘100’) on normal  
 468 scale; (b) talking (i.e. prolonged counting from ‘1’ to ‘100’) on logarithmic scale; (c) coughing  
 469 once on normal scale; (d) coughing once on logarithmic scale.

470  
 471 *3.4 LS exposure ratio*

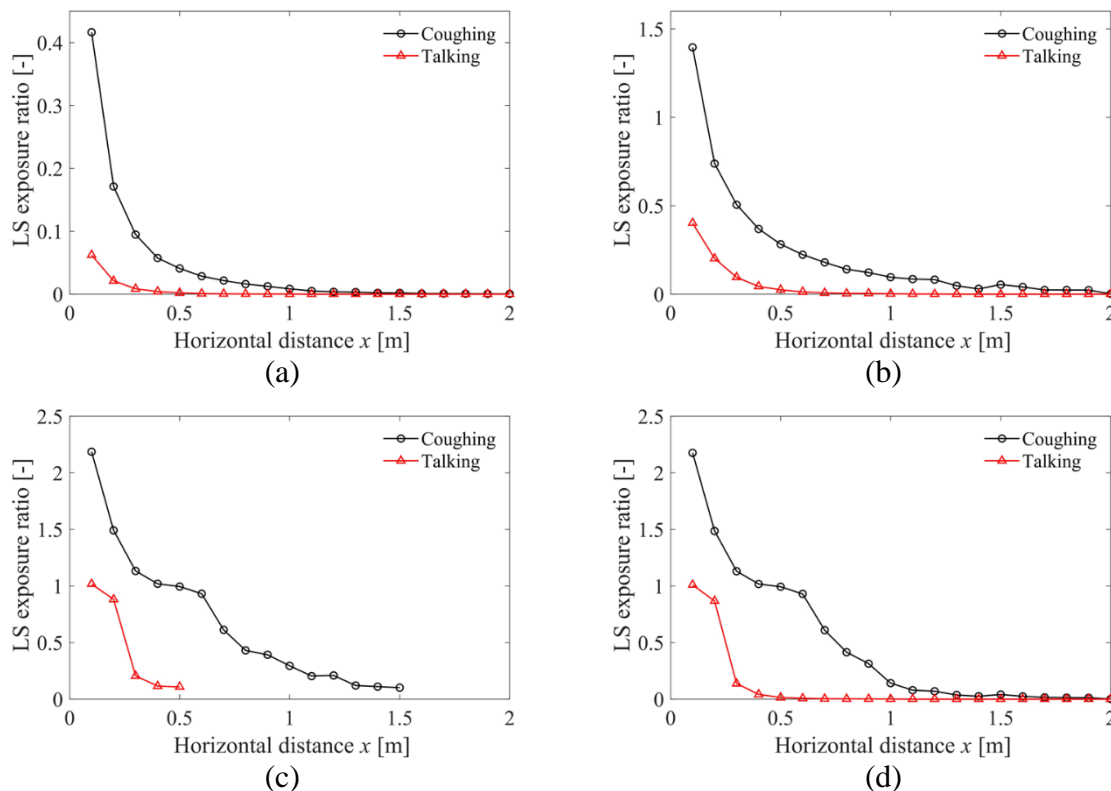
472 An *LS* ratio greater than unity (1) reveals a more significant role of the large droplet route. To  
 473 better understand the influences of different droplet sizes, we subdivided the initial droplet  
 474 size range into three segments for analysing *LS* exposure ratio: fine droplets smaller than 50  
 475  $\mu\text{m}$ , intermediate droplets between 50 and 100  $\mu\text{m}$  and large droplets greater than 100  $\mu\text{m}$ .  
 476 Note that this classification differs from what we defined earlier (small  $<75$   $\mu\text{m}$ , medium 75-  
 477 400  $\mu\text{m}$ , very large  $>400$   $\mu\text{m}$ ) in the analysis of travel distance. The *LS* ratio is shown as a  
 478 function of distance in Figure 8. For the large droplet group, the exposure risk by the large  
 479 droplet and/or short-range airborne routes dropped to zero beyond 0.5 m and 1.5 m for  
 480 talking and coughing, respectively. Therefore, in Figure 8c, the data do not span the entire

481 distance. The last two plots (c) and (d) are nearly identical, indicating that the large droplets  
 482 dominate the overall exposure. This is to be expected because the droplet volume is  
 483 proportional to the cube of droplet diameter, and thus the volume of a 750  $\mu\text{m}$  droplet is  
 484  $1.56 \times 10^7$  times that of a 3  $\mu\text{m}$  droplet. Figures 8a-c show that for larger droplets, the short-  
 485 range airborne route becomes less important, as the  $LS$  ratio increases with droplet size. The  
 486  $LS$  ratio exhibited a quasi-exponential decay for droplets smaller than 100  $\mu\text{m}$ , whilst for  
 487 large droplets the ratio showed more fluctuation. A plateau from 0.4-0.6 m was notable. In  
 488 this range, the inhalation zone diameter begins to experience a slower growth rate (Figure  
 489 B4). For large droplets in Figure 8c-d, the averaged vertical coordinate is still within mouth;  
 490 nevertheless, from 0.6 m on, they began to fall out of it. The fluctuation of the  $LS$  ratio for  
 491 large droplets may also be due to the uneven initial droplet-size distribution in this range, as  
 492 illustrated in Figure 2.

493

494 The results obtained for the whole droplet size range in Figure 8d are interesting. We can  
 495 conclude that the large droplet route is only dominant for talking within 0.2 m and for  
 496 coughing within 0.5 m. The short-range airborne is much more important at the remainder of  
 497 the close ranges studied here.

498



499 **Figure 8.**  $LS$  ratio for (a)  $<50 \mu\text{m}$ ; (b)  $50\text{-}100 \mu\text{m}$ ; (c)  $>100 \mu\text{m}$  (0.1-0.5 m for talking and 0.1-  
 500 1.5 m for coughing); (d) all sizes of droplets. Note: different vertical axis ranges are used.

501

## 502 4. Discussion

503

### 504 4.1 The short-range airborne sub-route dominates the close contact transmission

505 Our calculation shows that in contradiction to what is commonly believed, intermediate and  
 506 large droplets (including categories: 50 to 100  $\mu\text{m}$  and  $>100 \mu\text{m}$ ) are much less likely to be  
 507 deposited on the lip/eye/nosril mucosa of a susceptible person than to be inhaled, unless the  
 508 two are in very close contact. For the ideal situation that we have considered, the sphere

509 within which large droplets dominate deposition is 0.2 m for talking and approximately 0.5 m  
510 for coughing. In all other situations, the short-range airborne route dominates exposure. The  
511 inhalation area is much larger for talking than coughing, which explains why the talking-  
512 induced short-range airborne route is more important than that for coughing (Figure B4). The  
513 difference in inhalation zone areas directly affects the membrane/inhalation ratio.

514  
515 Reviewing the literature on large droplet transmission, one can find no direct evidence for  
516 large droplets as the route of transmission of any disease. It is known that the infection risk of  
517 many respiratory infections becomes higher when people come into closer contact. Flügge [6]  
518 pioneered the concept of large droplet transmission. He found that expiratory droplets  
519 contained bacteria and could not travel more than 1 or 2 m. Flügge [6] concluded that the  
520 expired droplets ‘settled out in short distances and in brief time intervals, airborne infection  
521 seemed almost eliminated’ [47]. The large droplet route became widely accepted after Chapin  
522 [7] developed his theory of the dominant contact transmission. Atkinson and Wein [24]  
523 suggested that large droplet transmission is less likely than formerly believed because close  
524 and unprotected exposure to direct expired air streams is rare. Our analysis disagrees with  
525 this point of view, instead showing that the insignificant role of large droplet transmission is  
526 due to the low rate of deposition even when direct expired air streams do exist.

527  
528 It seems that we are the first to consider the dependence of the deposition behaviour on the  
529 Stokes number and that of the inhalation probability on the aspiration efficiency. Although  
530 these are important physical parameters of close contact exposure, they were not considered  
531 in previous studies.

532  
533 Our work clearly shows that exposure due to the short-range airborne route dominates the  
534 overall exposure risk for droplets smaller than 50  $\mu\text{m}$ . Note that our calculation of exposure is  
535 based on droplet volumes only. In directly comparing the two exposures for the purpose of  
536 discussing infection risk, we implicitly assume that the virus concentrations are the same in  
537 all sizes of droplets, which is unlikely. Indeed, one common supporting argument for large  
538 droplet transmission is that large droplets contain most of the infectious viruses, whilst fine  
539 droplets do not. This was recently found to be untrue: instead, studies have shown that  
540 smaller droplets have higher virus concentrations than larger droplets [48-49]. Zhou et al.  
541 [50], in experiments on captive ferrets, found that droplets less than 1  $\mu\text{m}$  were not infectious,  
542 whilst those from 2 to 6  $\mu\text{m}$  did transmit infection; larger droplets were not identified. The  
543 droplet sizes (after evaporation) considered in those studies were all very small. The most  
544 relevant droplet size range in this study is thus 0 to 50  $\mu\text{m}$  (Figure 8a). In this range, the  
545 exposure due to the short-range airborne sub-route would be more than 2 times that due to  
546 large droplets even at a close distance of 0.1 m for coughing. For a typical inter-personal  
547 distance of 0.7 m [3], the same ratio for coughing becomes over 45. Note that we only  
548 compared the two sub-routes for talking and coughing separately, without considering the  
549 relative frequency of these respiratory activities. Face-to-face coughing is a rare event [24].  
550 There is a need to test the variability in the concentration of viable viruses in expired air  
551 streams. For this purpose, new, more efficient samplers that can better preserve virus activity  
552 are necessary [48, 51].

#### 553 4.2 Threshold droplet size for large droplet is not 5 or 10 $\mu\text{m}$ , but 50-100 $\mu\text{m}$

554 Our calculation of the deposition efficiency clearly shows that droplets smaller than 100  $\mu\text{m}$   
555 are less likely to be deposited on the facial parts of the susceptible person (Figure 8),  
556 although it is not the main purpose of this paper to calculate the large droplet threshold size.  
557 However, this is an important concept that is relevant to our discussion of the dominant sub-  
558

559 route. In [Figure 8](#), droplets at the point of release (i.e. mouth) are divided into three ranges:  
560 fine droplets (0-50  $\mu\text{m}$ ), intermediate sizes (50-100  $\mu\text{m}$ ) and large droplets (>100  $\mu\text{m}$ ). For  
561 the size range 0 to 50  $\mu\text{m}$ , the droplets will be airborne in the expired air streams for the time  
562 scales that we consider here, particularly after evaporation.

563  
564 Our calculation confirms that the size-dependent difference in the deposition efficiency of  
565 droplets on the face is one of the major reasons for the calculated differences between the two  
566 exposure routes. Droplets in the small size group (<75  $\mu\text{m}$ ), which can closely follow the air  
567 stream, have relatively low Stokes numbers and are unlikely to be deposited. The medium  
568 size group (75-400  $\mu\text{m}$ ) would land on the ground the soonest. Droplets in the very large size  
569 group (>400  $\mu\text{m}$ ) have the greatest potential for facial deposition and travel the greatest  
570 distance before falling to the ground.

571  
572 Thus, the commonly assumed threshold droplet size of 5 or 10  $\mu\text{m}$  is not only wrong, but  
573 intrinsically misleading. This assumption leads to the false conclusion that droplet  
574 transmission only applies to droplets larger than 5  $\mu\text{m}$ . Our literature review shows that it was  
575 probably Garner et al. [52] who first suggested this droplet transmission lower boundary of 5  
576  $\mu\text{m}$ , without citing any reference. The WHO 2014 guideline [53] still defines droplets as  
577 ‘respiratory aerosols > 5  $\mu\text{m}$  in diameter’. Siegel et al. [54] recognised that ‘observations of  
578 particle dynamics have demonstrated that a range of droplet sizes, including those with  
579 diameters of 30  $\mu\text{m}$  or greater, can remain suspended in the air’. We distinguished the two  
580 sub-routes known as “large droplet” and “short-range airborne” according to the way the  
581 susceptible was exposed to (i.e., deposition and inhalation) in this study, and our determined  
582 size range also differs from the traditional droplet size range. Traditional term such as large  
583 droplet transmission may be misleading. However, more effort would be necessary for  
584 recognizing the threshold droplet size, and the precise transmission route(s) need to be  
585 reconsidered as more data become available.

586  
587 *4.3 Assumption of the dominant large droplet sub-route may hinder development and*  
588 *acceptance of alternative interventions*

589 The effectiveness of surgical masks depends on the dominance of large-droplet transmission  
590 by droplets greater than 50  $\mu\text{m}$  in diameter. A number of studies have questioned their  
591 effectiveness against influenza. Milton et al. [48] found that surgical masks could reduce viral  
592 copy numbers by 25-fold for droplets larger than 5  $\mu\text{m}$  but only 2.8-fold for fine droplets  
593 smaller than 5  $\mu\text{m}$ . The use of facemasks itself is not detrimental, but reflects a strong belief  
594 in the dominant role of large droplet transmission, due to which other possible interventions  
595 are likely to be neglected.

596  
597 Mechanistically, the use of surgical masks by an infected can ‘block’ or ‘kill’ expiratory jets;  
598 that is, the expired air is initially blocked within the facial cavity of the mask of the infected  
599 before eventually leaking out to the environment through the mask itself or the gaps on either  
600 side. The momentum of the blocked expired jet becomes so weak that it is most likely to be  
601 captured by the body plume of the infected. The body plume carries the weakened expired  
602 stream into the upper level of the indoor space, which eventually becomes a part of the room  
603 air, contributing to the long-range airborne route, which is expected to be much weaker than  
604 the short-range airborne route.

605  
606 Importantly, the expired air streams have a velocity much greater than the typical indoor air  
607 flows (0.2 m/s), hence the room air flows do not significantly alter the expired jet trajectory.  
608 Hence, general ventilation cannot prevent transmission by the short-range airborne route [9].

609 Personalised ventilation systems may be effective here because they provide filtered and safe  
610 air directly to the breathing zone of the susceptible person [55-57]. Personalised ventilation  
611 devices can be installed at fixed places such as office chairs, desks or computers, enabling  
612 occupants to control its temperature, flow rate and direction [55]. However, for people  
613 without fixed workplace, no existing ventilation strategy is currently available for mitigating  
614 the short-range airborne route, and innovative new ideas are needed.

615

#### 616 *4.4 Difference between the short-range airborne and large droplet route*

617 In this study, we considered the short-range airborne route and the large droplet route  
618 separately as two processes. The susceptible person was assumed to hold his or her breath  
619 with mouth open for the large droplet route and inhale orally for the short-range airborne  
620 route. The situation of coexistence of the two routes was also calculated, where an imaginary  
621 plane at the target mouth was responsible for the large droplet sub-route; see [Appendix A](#) for  
622 a summary of the important results.

623

624 It is important to uncover the mechanistic details of the difference between the airborne and  
625 large droplet routes. The fate of droplets after entering the human body through respiratory  
626 activities seems to depend on their size. Different droplet sizes lead to differences in  
627 deposition efficiency at different sites (i.e., head airways, tracheobronchial region or alveolar  
628 region) [58]. According to Carvalho et al. [59], particles between 1 and 5  $\mu\text{m}$  are deposited  
629 deep in the lungs, whilst those larger than 10  $\mu\text{m}$  are generally deposited in the oropharyngeal  
630 region, and particles smaller than 1  $\mu\text{m}$  are exhaled. The response dose can also be region-  
631 sensitive for drug delivery [60] and potential hazard [61]. If we consider the final fate of  
632 infectious droplets, their destiny is deposition, whether in the head airways or in alveoli, via  
633 inertia impaction, sedimentation or diffusion. The relative probabilities of the short-range  
634 airborne route and the large droplet route may depend on processes external to the body,  
635 implying that disease prevention measures should focus on the ambient air streams.

636

637 We focused on the jet and droplet dynamics outside the human body in this study. The large  
638 droplet and short-range airborne routes become indistinguishable at the target mouth plane  
639 when considering both sub-routes simultaneously. As shown by Anthony and Flynn [11]  
640 using CFD, particles larger than 5  $\mu\text{m}$  can be deposited on the inside surface of the lips due to  
641 gravity settling. If such a CFD approach is used, one may define inhalation more precisely by  
642 only including those particles that go through the area ‘between the lips’. Here we considered  
643 all particles that were ‘directed toward the mouth’ [11], which may be the upper bound of  
644 aspiration by inhalation. When a droplet passes through the mouth orifice, we cannot  
645 rigorously determine whether it is due to deposition or inhalation, which makes it  
646 meaningless to attempt to distinguish between them at the mouth plane. We therefore  
647 presented the results of the large droplet and short-range airborne routes as two separate  
648 processes in the main text. Note that when the two sub-routes co-exist ([Appendix A](#)), the  
649 major difference from the situations presented in the main text is that once a particle is  
650 inhaled, the particle is no longer available for deposition. The predicted range of dominance  
651 of the short-range airborne route was extended slightly to 0.3 m for talking and 0.9 m for  
652 coughing ([Appendix A](#)), although large droplet route becomes more important in the  
653 coexistence case. However, a more careful redefinition of the short-range airborne route and  
654 the large droplet route will require additional data.

655

#### 656 *4.5 Limitations of the study*

657 Despite the valuable findings, our study still has the following limitations.

658

659 First, exposure ( $\mu\text{L}$ ) was used as the criterion of infection based on the assumption that every  
660 unit volume of droplet contains the same amount of activated viruses. Nevertheless,  
661 according to Lindsley et al. [62], most (~65%) virus RNA was contained in droplets smaller  
662 than  $4\ \mu\text{m}$  expelled by coughing, which indicates a higher risk in the respiratory range.  
663 Although the exclusion of droplets smaller than  $3\ \mu\text{m}$  would exert negligible influence on  
664 exposure given their small droplet volume, significant implications may exist when virus  
665 concentration variation is considered. The critical infective dose was also not considered.  
666 Future work could be done from a more biologically informed perspective based on the  
667 exposure results. Second, the number of simulated droplets was relatively small. Because *MF*  
668 and *IF* are statistical probability values, a larger number of droplets, if possible, would give  
669 more robust results. Third, the worst-case scenario of mouth inhalation and that of deposition  
670 were studied, which may deviate slightly from realistic situations. Such worst scenarios might  
671 occur during face to face conversations, but data on the frequency of its occurrence is not  
672 available. Although the effects associated with nose-versus-mouth breathing and facial  
673 structural features are weak [36], a more detailed nose inhalation model is still desirable. Our  
674 two nostrils are very close to each other, and they mostly face downward at a certain angle.  
675 During the nasal inhalation, the configuration of the inhalation zone would be distorted by  
676 one another. Exposure due to both inhalation and deposition was estimated using existing  
677 empirical formulas assuming a spherical head shape. Other factors like relative subject  
678 height, face-to-face angle and mouth covering may greatly affect the exposure results.  
679 Different indoor airflow patterns due to different air distribution strategies and human body  
680 thermal plumes, which can disperse droplets, would also cause discrepancies, especially at  
681 farther distances. Improved experiments and CFD simulations are needed to investigate the  
682 influence of potential factors under more realistic contexts.

683  
684 Finally, only two transmission routes were considered in our work. Because the mucous  
685 membranes are small in area relative to the total frontal area of the head, most exhaled  
686 droplets are likely deposited on other regions like cheeks, neck or hair. These deposited  
687 droplets might be touched by the susceptible person's own hands, which subsequently touch  
688 his or her mucosa, resulting in self-inoculation. Recent data by Zhang et al. [63] show that  
689 people touch their face very frequently. Facial deposition and touch may contribute another  
690 potential transmission route in close contact, which is worth exploring in future.

## 691 692 **5. Conclusions**

693  
694 This is probably the first study in which the large droplet route, traditionally believed to be  
695 dominant, has been shown to be negligible compared with the short-range airborne route, at  
696 least for expired droplets smaller than  $100\ \mu\text{m}$  in size at the mouth of the infected. The  
697 exposure due to short-range airborne transmission surpasses that of the former route in most  
698 situations for both talking and coughing. The large droplet route only dominates when the  
699 droplets are larger than  $100\ \mu\text{m}$ , within  $0.2\ \text{m}$  for talking and  $0.5\ \text{m}$  for coughing. The smaller  
700 the exhaled droplets, the more important the short-range airborne route. The large droplet  
701 route contributes less than 10% of exposure when the droplets are less than  $50\ \mu\text{m}$  at a  
702 distance greater than  $0.3\ \text{m}$ , even for coughing. For the direct face-to-face configuration,  
703 exhaled air streams begin to cover the nostrils of the susceptible person from  $0.2$  to  $0.3\ \text{m}$  and  
704 the eyes from  $0.4$  to  $0.5\ \text{m}$ . While talking, more droplets are deposited on the eyes at long  
705 distances due to a larger jet trajectory curvature (Appendix B). Exposure decreases as the  
706 interpersonal distance increases for both large droplet and short-range airborne sub-routes.

707  
708 Short-range airborne transmission is dominant beyond  $0.2\ \text{m}$  for talking and  $0.5\ \text{m}$  for

709 coughing. Within the 2-m interpersonal distance, the shortest distance is travelled by droplets  
710 of approximately 112.5 to 225  $\mu\text{m}$  in size for talking and 175 to 225  $\mu\text{m}$  for coughing. The  
711 smaller droplets follow the indoor air stream, whilst the larger droplets are dominated by their  
712 inertia and travel a longer distance.

713  
714 The work presented here poses a challenge to the traditional belief that large droplet infection  
715 is dominant. Because the short-range airborne route is dominant for both talking and  
716 coughing according to the results here, novel methods of personalised ventilation during  
717 close contact are worth considering as a strategy for disease control.

718

### 719 *Acknowledgements*

720 This work was supported by a General Research Fund (grant number 17202719) and  
721 Collaborative Research Fund (grant number C7025-16G), both provided by the Research  
722 Grants Council of Hong Kong.

723

### 724 **Conflict of Interest Statement**

725 The authors declare no conflict of interest.

726

### 727 *References*

728

- 729 [1] J. Wei, Y. Li, Airborne spread of infectious agents in the indoor environment, *Am. J.*  
730 *Infect. Control* 44 (9) (2016) S102-S108.
- 731 [2] G. Brankston, L. Gitterman, Z. Hirji, C. Lemieux, M. Gardam, Transmission of influenza  
732 A in human beings, *Lancet Infect. Dis.* 7 (4) (2007) 257-265.
- 733 [3] N. Zhang, J.W. Tang, Y. Li, Human behavior during close contact in a graduate student  
734 office, *Indoor air* 29 (4) (2019) 577-590.
- 735 [4] A. Pease, *Body language: How to read others' thoughts by their gestures*, Sheldon Press,  
736 London, 1984.
- 737 [5] J.M. Villafruela, I. Olmedo, J.F. San José, Influence of human breathing modes on  
738 airborne cross infection risk, *Build. Environ.* 106 (2016) 340-351.
- 739 [6] C. Flügge, Ueber luftinfection, *Med. Microbiol. Immunol.* 25 (1) (1897) 179-224.
- 740 [7] C.V. Chapin, *The Sources and Modes of Infection*, John Wiley & Sons, New York, 1912.
- 741 [8] K. Han, X. Zhu, F. He, L. Liu, L. Zhang, et al., Lack of airborne transmission during  
742 outbreak of pandemic (H1N1) 2009 among tour group members, China, June 2009,  
743 *Emerg. Infect. Dis* 15 (10) (2009) 1578-1581.
- 744 [9] L. Liu, Y. Li, P.V. Nielsen, J. Wei, R.L. Jensen, Short-range airborne transmission of  
745 expiratory droplets between two people, *Indoor Air* 27 (2) (2017) 452-462.
- 746 [10] J.H. Vincent, Health-related aerosol measurement: a review of existing sampling criteria  
747 and proposals for new ones, *J. Environ. Monit.* 7 (11) (2005) 1037-1053.
- 748 [11] T.R. Anthony, M.R. Flynn, Computational fluid dynamics investigation of particle  
749 inhalability, *J. Aerosol. Sci.* 37 (6) (2006) 750-765.
- 750 [12] J. Kim, J. Xi, X. Si, A. Berlinski, W.C. Su, Hood nebulization: effects of head direction  
751 and breathing mode on particle inhalability and deposition in a 7-month-old infant  
752 model, *J. Aerosol Med. Pulm. Drug Deliv.* 27 (3) (2014) 209-218.
- 753 [13] S. Erdal, N.A. Esmert, Human head model as an aerosol sampler: calculation of  
754 aspiration efficiencies for coarse particles using an idealized human head model facing  
755 the wind, *J. Aerosol. Sci.* 26 (2) (1995) 253-272.
- 756 [14] F.A. Berlanga, M.R. de Adana, I. Olmedo, J.M. Villafruela, J.F. San José, et al.,  
757 Experimental evaluation of thermal comfort, ventilation performance indices and  
758 exposure to airborne contaminant in an airborne infection isolation room equipped with a

- 759 displacement air distribution system, *Energy Build.* 158 (2018) 209-221.
- 760 [15] J.K. Gupta, C.H. Lin, Q. Chen, Characterizing exhaled airflow from breathing and  
761 talking, *Indoor Air* 20 (1) (2010) 31-39.
- 762 [16] L.J.G.R. Morawska, G.R. Johnson, Z.D. Ristovski, M. Hargreaves, K. Mengersen, et al.,  
763 Size distribution and sites of origin of droplets expelled from the human respiratory tract  
764 during expiratory activities, *J. Aerosol. Sci.* 40 (3) (2009) 256-269.
- 765 [17] J.P. Duguid, The size and the duration of air-carriage of respiratory droplets and droplet-  
766 nuclei, *Epidemiol. Infect.* 44 (6) (1946) 471-479.
- 767 [18] C. Xu, P.V. Nielsen, G. Gong, L. Liu, R.L. Jensen, Measuring the exhaled breath of a  
768 manikin and human subjects, *Indoor Air* 25 (2) (2015) 188-197.
- 769 [19] J.H.W. Lee, V. Chu, *Turbulent jets and plumes: a Lagrangian approach*, Springer Science  
770 & Business Media, New York, 2012.
- 771 [20] J. Wei, Y. Li, Enhanced spread of expiratory droplets by turbulence in a cough jet, *Build.*  
772 *Environ.* 93 (2015) 86-96.
- 773 [21] C.Y.H. Chao, M.P. Wan, L. Morawska, G.R. Johnson, Z.D. Ristovski, et al.,  
774 Characterization of expiration air jets and droplet size distributions immediately at the  
775 mouth opening, *J. Aerosol. Sci.* 40 (2) (2009) 122-133.
- 776 [22] T.A. Popov, S. Dunev, T.Z. Kralimarkova, S. Kraeva, L.M. DuBuske, Evaluation of a  
777 simple, potentially individual device for exhaled breath temperature measurement,  
778 *Respir. Med.* 101 (10) (2007) 2044-2050.
- 779 [23] V.V.E. Baturin, *Fundamentals of Industrial Ventilation*, Pergamon Press, Oxford, 1972.
- 780 [24] M.P. Atkinson, L.M. Wein, Quantifying the routes of transmission for pandemic  
781 influenza, *Bull. Math. Biol.* 70 (3) (2008) 820-867.
- 782 [25] M. Nicas, R.M. Jones, Relative contributions of four exposure pathways to influenza  
783 infection risk, *Risk Anal.* 29 (9) (2009) 1292-1303.
- 784 [26] U. EPA, *Exposure Factors Handbook 2011 Edition (Final)*, US Environmental Protection  
785 Agency, Washington, DC, 2011.
- 786 [27] E. Hjelmås, B.K. Low, Face detection: A survey, *Comput. Vis. Image Underst.* 83 (3)  
787 (2001) 236-274.
- 788 [28] I. Langmuir, K.B. Blodgett, A mathematical investigation of water droplet trajectories,  
789 *Army Air Forces Technical Report* 5418, 1946.
- 790 [29] W.H. Walton, A. Woolcock, in: E.G. Richardson (Ed.), *Aerodynamic Capture of*  
791 *particles*, Pergamon Press, New York, 1960, pp. 129-153.
- 792 [30] F. Hähner, G. Dau, F. Ebert, Inertial impaction of aerosol particles on single and multiple  
793 spherical targets, *Chem. Eng. Technol.* 17 (2) (1994) 88-94.
- 794 [31] M. Waldenmaier, Measurements of inertial deposition of aerosol particles in regular  
795 arrays of spheres, *J. Aerosol. Sci.* 30 (10) (1999) 1281-1290.
- 796 [32] T.L. Ogden, J.L. Birkett, The human head as a dust sampler, in: W.H. Walton (Ed.),  
797 *Inhaled particles IV*, Pergamon Press, Oxford, 1977, pp. 93-105.
- 798 [33] L. Armbruster, H. Breuer, Investigations into defining inhalable dust, in: W.H. Walton  
799 (Ed.), *Inhaled particles V*, Pergamon Press, Oxford, 1982, pp. 21-32.
- 800 [34] J.H. Vincent, D. Mark, Applications of blunt sampler theory to the definition and  
801 measurement of inhalable dust, in: W.H. Walton (Ed.), *Inhaled particles V*, Pergamon  
802 Press, Oxford, 1982, pp. 3-19.
- 803 [35] R.J. Aitken, P.E.J. Baldwin, G.C. Beaumont, L.C. Kenny, A.D. Maynard, Aerosol  
804 inhalability in low air movement environments, *J. Aerosol. Sci.* 30 (5) (1999) 613-626.
- 805 [36] J.H. Vincent, D. Mark, B.G. Miller, L. Armbruster, T.L. Ogden, Aerosol inhalability at  
806 higher windspeeds, *J. Aerosol. Sci.* 21 (4) (1990) 577-586.
- 807 [37] D.J. Hsu, D.L. Swift, The measurements of human inhalability of ultralarge aerosols in  
808 calm air using mannikins, *J. Aerosol. Sci.* 30 (10) (1999) 1331-1343.



- 809 [38] W.C. Su, J.H. Vincent, Towards a general semi-empirical model for the aspiration  
810 efficiencies of aerosol samplers in perfectly calm air, *J. Aerosol. Sci.* 35 (9) (2004) 1119-  
811 1134.
- 812 [39] S.J. Dunnett, D.B. Ingham, The human head as a blunt aerosol sampler, *J. Aerosol. Sci.*  
813 19 (3) (1988a) 365-380.
- 814 [40] T.R. Anthony, Contribution of facial feature dimensions and velocity parameters on  
815 particle inhalability, *Ann. Occup. Hyg.* 54 (6) (2010) 710-725.
- 816 [41] S.J. Dunnett, D.B. Ingham, An empirical model for the aspiration efficiencies of blunt  
817 aerosol samplers orientated at an angle to the oncoming flow, *Aerosol Sci. Technol.* 8 (3)  
818 (1988b) 245-264.
- 819 [42] S. Zhu, S. Kato, J.H. Yang, Study on transport characteristics of saliva droplets produced  
820 by coughing in a calm indoor environment, *Build. Environ.* 41 (12) (2006) 1691-1702.
- 821 [43] W. Sun, J. Ji, Transport of droplets expelled by coughing in ventilated rooms, *Indoor*  
822 *Built Environ.* 16 (6) (2007) 493-504.
- 823 [44] W.F. Wells, On air-borne infection: study II. droplets and droplet nuclei, *Am. J.*  
824 *Epidemiol.* 20 (3) (1934) 611-618.
- 825 [45] X. Xie, Y. Li, A.T. Chwang, P.L. Ho, W.H. Seto, How far droplets can move in indoor  
826 environments--revisiting the Wells evaporation-falling curve, *Indoor air* 17 (3) (2007)  
827 211-225.
- 828 [46] J.Y. Hsu, R.A. Stone, R.B. Logan-Sinclair, M. Worsdell, C.M. Busst, et al., Coughing  
829 frequency in patients with persistent cough: assessment using a 24 hour ambulatory  
830 recorder, *Eur. Resp. J.* 7 (7) (1994) 1246-1253.
- 831 [47] W.F. Wells, M.W. Wells, Air-borne infection, *JAMA-J. Am. Med. Assoc.* 107 (21)  
832 (1936) 1698-1703.
- 833 [48] D.K. Milton, M.P. Fabian, B.J. Cowling, M.L. Grantham, J.J. McDevitt, 2013. Influenza  
834 virus aerosols in human exhaled breath: particle size, culturability, and effect of surgical  
835 masks. *PLoS Pathog.* 9 (3), e1003205.
- 836 [49] J. Yan, M. Grantham, J. Pantelic, P.J.B. de Mesquita, B. Albert, et al., Infectious virus in  
837 exhaled breath of symptomatic seasonal influenza cases from a college community, *Proc.*  
838 *Natl. Acad. Sci. U. S. A.* 115 (5) (2018) 1081-1086.
- 839 [50] J. Zhou, J. Wei, K.T. Choy, S.F. Sia, D.K. Rowlands, et al., Defining the sizes of  
840 airborne particles that mediate influenza transmission in ferrets, *Proc. Natl. Acad. Sci. U.*  
841 *S. A.* 115 (10) (2018) E2386-E2392.
- 842 [51] P. Fabian, J.J. McDevitt, E.A. Houseman, D.K. Milton, Airborne influenza virus  
843 detection with four aerosol samplers using molecular and infectivity assays:  
844 considerations for a new infectious virus aerosol sampler, *Indoor Air* 19 (5) (2009) 433-  
845 441.
- 846 [52] J.S. Garner, Hospital Infection Control Practices Advisory Committee, Guideline for  
847 isolation precautions in hospitals, *Infect. Control Hosp. Epidemiol.* 17 (1) (1996) 54-80.
- 848 [53] World Health Organization (WHO), Infection prevention and control of epidemic-and  
849 pandemic-prone acute respiratory infections in health care, Geneva, WHO, 2014.
- 850 [54] J.D. Siegel, E. Rhinehart, M. Jackson, L. Chiarello, Health Care Infection Control  
851 Practices Advisory Committee, 2007 Guideline for isolation precautions preventing  
852 transmission of infectious agents in healthcare settings, *Am. J. Infect. Control* 35 (Suppl.  
853 2) (2007) S65-S164.
- 854 [55] A.K. Melikov, Personalized ventilation, *Indoor air* 14 (2004) 157-167.
- 855 [56] J. Niu, N. Gao, M. Phoebe, Z. Huigang, Experimental study on a chair-based  
856 personalized ventilation system, *Build. Environ.* 42 (2) (2007) 913-925.
- 857 [57] J. Pantelic, G.N. Sze-To, K.W. Tham, C.Y. Chao, Y.C.M. Khoo, Personalized ventilation  
858 as a control measure for airborne transmissible disease spread, *J. R. Soc. Interface* 6

- 859 (Suppl. 6) (2009) S715-S726.  
860 [58] W.C. Hinds, Aerosol technology: properties, behavior, and measurement of airborne  
861 particles, John Wiley & Sons, New York, 1999.  
862 [59] T.C. Carvalho, J.I. Peters, R.O. Williams III, Influence of particle size on regional lung  
863 deposition—what evidence is there? *Int. J. Pharm.* 406 (1-2) (2011) 1-10.  
864 [60] J.N. Pritchard, The influence of lung deposition on clinical response, *J. Aerosol Med.* 14  
865 (Suppl. 1) (2001) S19-S26.  
866 [61] G.F.G. Bezemer, Particle deposition and clearance from the respiratory tract, Institute for  
867 Risk Assessment Sciences, University of Utrecht, The Netherlands, 2009.  
868 [62] W.G. Lindsley, F.M. Blachere, R.E. Thewlis, A. Vishnu, K.A. Davis, et al., 2010.  
869 Measurements of airborne influenza virus in aerosol particles from human coughs. *PLoS*  
870 *One* 5 (11), e15100.  
871 [63] N. Zhang, Y. Li, H. Huang, Surface touch and its network growth in a graduate student  
872 office, *Indoor air* 28 (6) (2018) 963-972.  
873

#### 874 ***Appendix A. Evaluation of LS ratio considering the coexistence of the two sub-routes***

875  
876 When considering the coexistence of the large droplet and short-range airborne routes, an  
877 imaginary plane was assumed at the target mouth. Droplets deposited on the plane were  
878 assigned to the large droplet route, and those filtering through it were assigned to short-range  
879 airborne transmission.

880  
881 The short-range airborne exposure is still calculated as:  
882

$$883 e_{SR}(x) = \sum_{i=1}^N n_{0i} \cdot v_{pi} \cdot IF_i \cdot AE_i \quad (A.1)$$

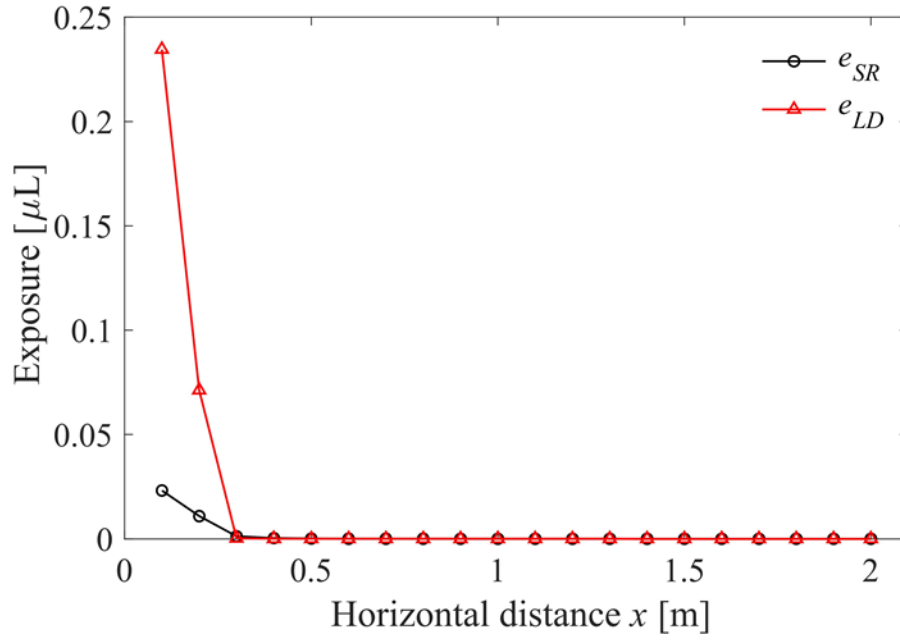
884  
885 When the large droplet route and short-range airborne route co-exist, the droplet deposition  
886 behaviours are expected to be affected by inhalation flow. Based on whether droplets exist  
887 simultaneously both on facial membranes and in the inhalation zone, we divided the large  
888 droplet exposure into two parts, where the total large droplet exposure is the sum of them.  
889  $e_{LD1}(x)$  represents the case when droplets are outside the inhalation zone, whilst  $e_{LD2}(x)$   
890 indicates that facial mucous membranes overlap with inhalation zone. The membrane fraction  
891 ( $MF$ ) and deposition efficiency ( $DE$ ) also change accordingly.

$$892$$
$$893 e_{LD1}(x) = \sum_{i=1}^N n_{0i} \cdot v_{pi} \cdot MF_{i1} \cdot DE_{i1} \quad (A.2)$$

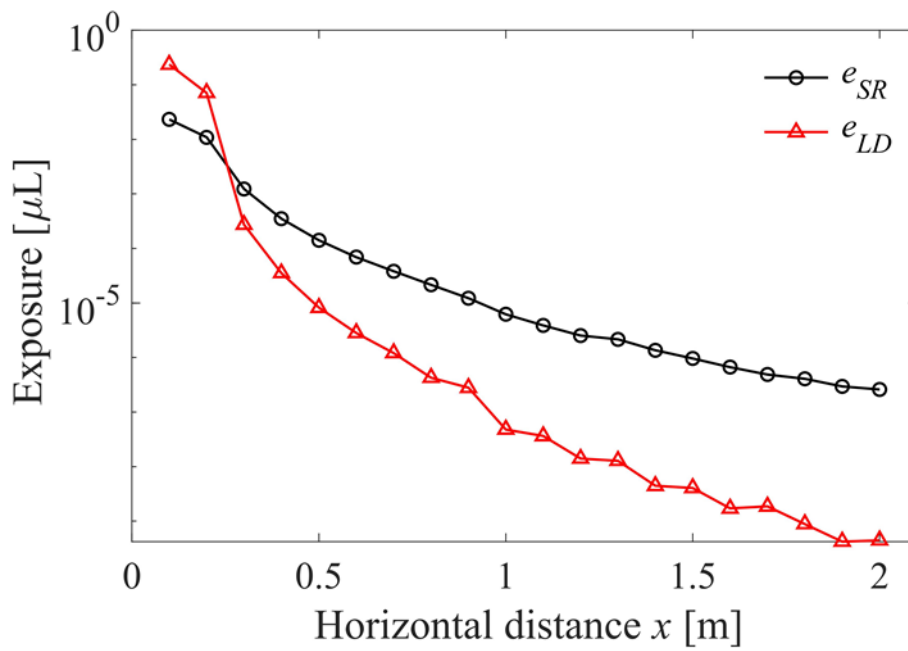
$$894 e_{LD2}(x) = \sum_{i=1}^N n_{0i} \cdot v_{pi} \cdot MF_{i2} \cdot DE_{i2} \quad (A.3)$$

895  
896  $DE_{i1}$  remains the same as defined in Equation (21). Unlike the original inhalation model, when  
897 the short-range airborne and large droplet routes co-exist, an imaginary plane is included at the  
898 target mouth. Therefore, we made a small change to the original model, such that  $DE_{i2}$  equals  
899  $\alpha_c$ , which is the impaction efficiency (Equation (28)). As  $AE_i$  and  $DE_{i2}$  affect each other in  
900 the convergent part of the air stream,  $AE_i$  equals  $1 - \alpha_c$  accordingly.  
901

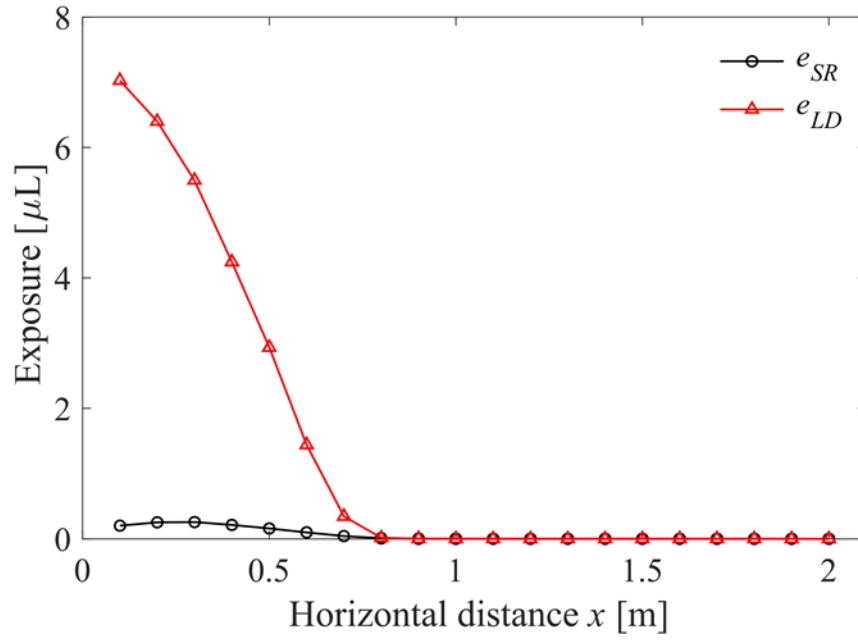
902 The results of the estimated total exposure and  $LS$  ratio are shown in Figure A1 and Figure A2  
903 respectively.



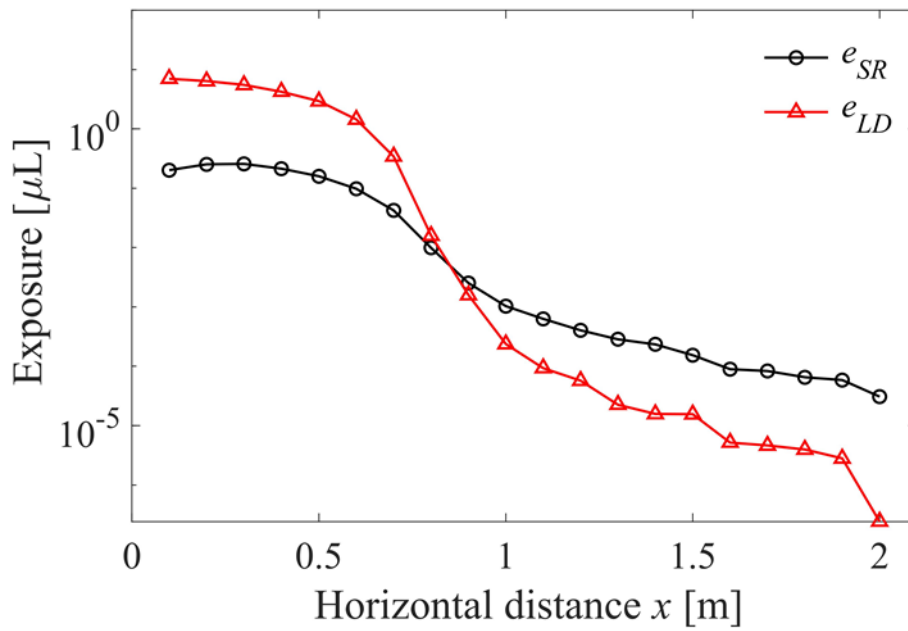
(a)



(b)

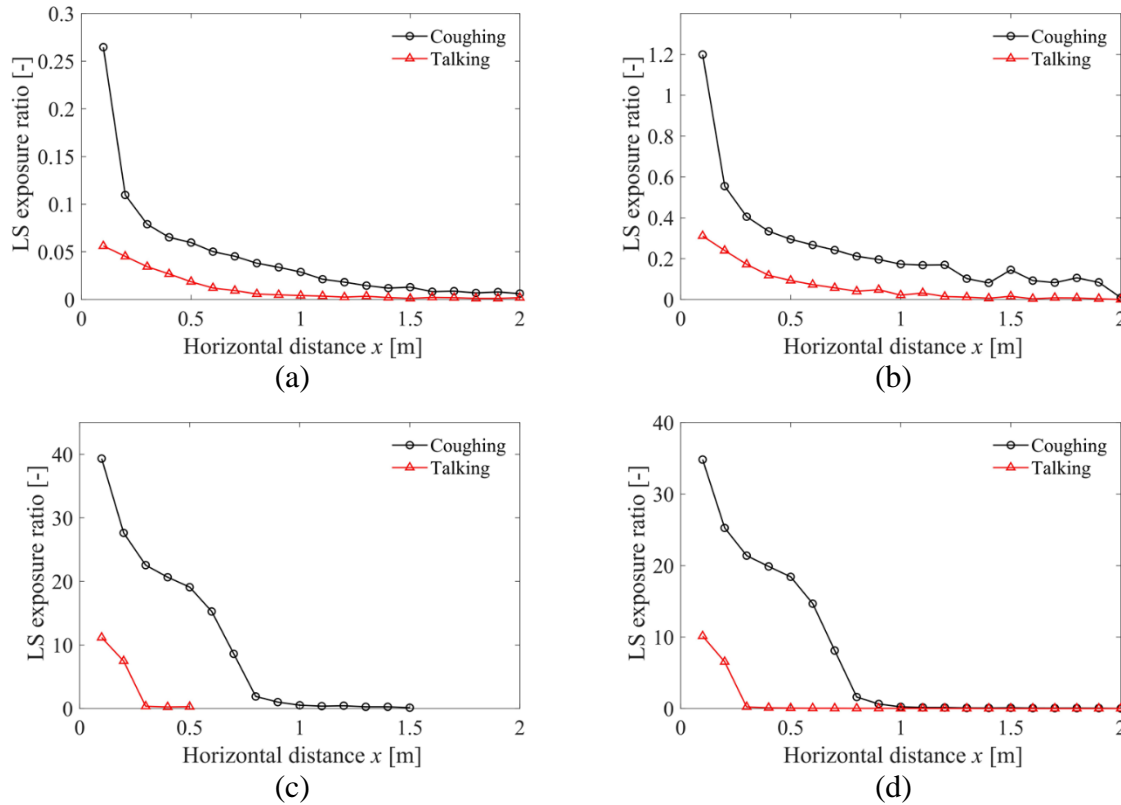


(c)



(d)

904  
905 **Figure A1.** Total exposure for (a) talking (i.e. prolonged counting from ‘1’ to ‘100’ once) on  
906 normal scale; (b) talking (i.e. prolonged counting from ‘1’ to ‘100’ once) on logarithmic scale;  
907 (c) coughing once on normal scale; (d) coughing once on logarithmic scale.  
908



909 **Figure A2.** *LS* ratio for (a)  $<50 \mu\text{m}$ ; (b)  $50\text{-}100 \mu\text{m}$ ; (c)  $>100 \mu\text{m}$  (0.1-0.5 m for talking and  
 910 0.1-1.5 m for coughing); (d) all sizes of droplets. Note different vertical axis ranges are used.

911

912 As a whole, the same trend was observed as in [Figure 8](#), although short-range airborne sub-  
 913 route becomes slightly more important for droplets smaller than  $100 \mu\text{m}$  while large droplet  
 914 route is dramatically more significant for those larger than  $100 \mu\text{m}$ . The *LS* ratio values for  
 915 talking/coughing all resemble each other for all droplet sizes, except that a slower decay was  
 916 observed for coughing from 0.3 to 0.5 m. In this range, the inhalation zone diameter begins to  
 917 experience a slower growth rate ([Figure B4](#)). For large droplets in [Figure A2c-d](#), the averaged  
 918 vertical coordinate is still within mouth; nevertheless, from 0.6 m on, they began to fall out of  
 919 it. The fluctuation of the *LS* ratio for large droplets may also be due to the uneven initial  
 920 droplet-size distribution in this range as illustrated in [Figure 2](#).

921

922

## 923 **Appendix B. Deposition and aspiration**

924

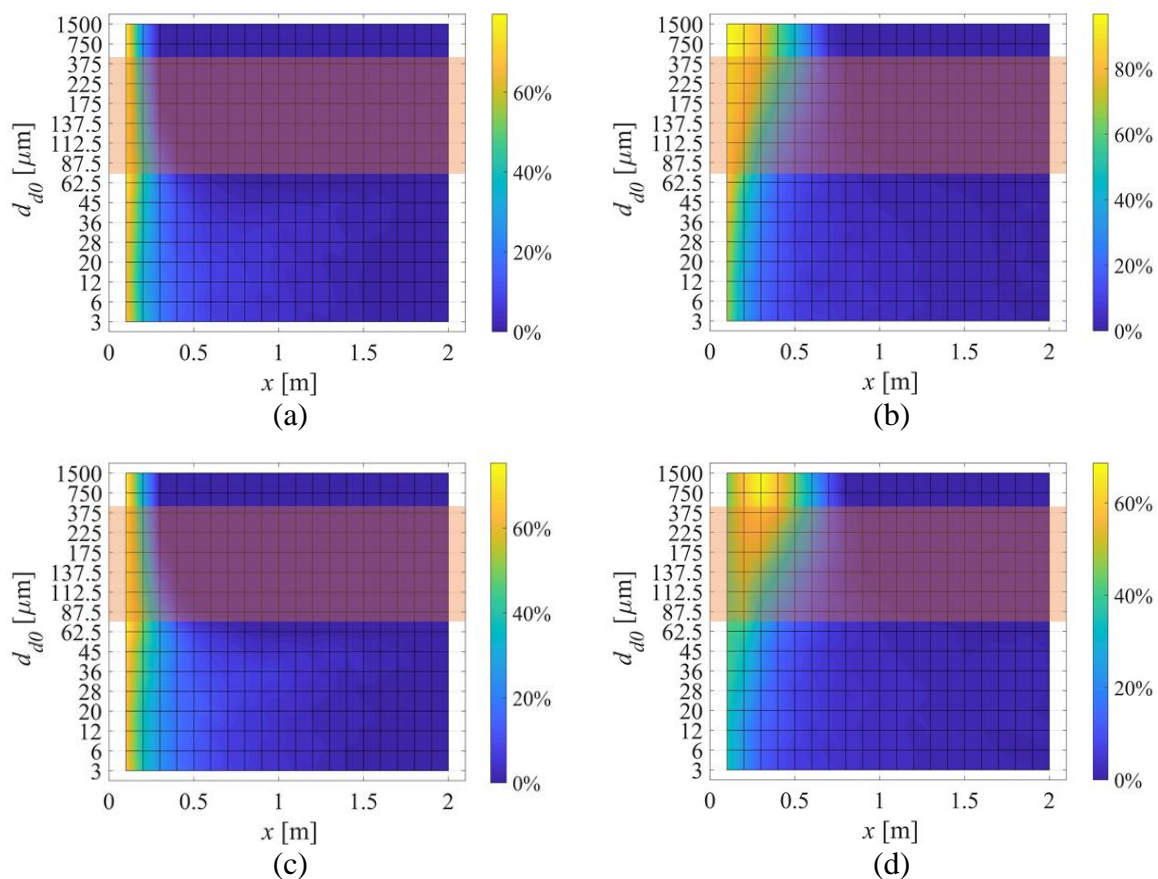
925 Statistically, our defined membrane fraction (*MF*) and inhalation fraction (*IF*) are case-  
 926 sensitive probabilities smaller than 1. The values differ with the relative height of the target  
 927 and source, face features, head direction and inhalation velocity. As mentioned above, the  
 928 worst-case scenario was considered in this study. For the current specific case, *MF* and *IF*  
 929 varied with distance and droplet size as demonstrated in [Figure B1](#). Note that different  
 930 legends are used. *MF* and *IF* dropped to approximately zero for large droplets at long  
 931 distance. [Figure B1c](#) and [d](#) show that the talking *IF* and coughing *IF* differ considerably at  
 932 close range ( $<0.5$  m). Although the values for talking were dispersed uniformly across the  
 933 whole size range, the maximum values appeared for large droplets, as highlighted at the left  
 934 top corner. The overall trend of *MF* resembles that of *IF* for both talking and coughing. This  
 935 indicates that higher exhalation velocities would affect the large droplet behaviours, which in  
 936 turn influences exposure. A clear boundary can be detected for both talking *IF* and talking

937 *MF*, where medium and large droplets begin to fall out of the jet region with a sharp decrease  
938 of their vertical coordinates. The critical size was around  $62.5 \mu\text{m}$ .

939  
940 The ratio of inhaled/deposited droplets for talking and coughing as a function of distance is  
941 shown in Figure B2. Inhaled droplets were one order of magnitude more numerous than  
942 deposited droplets, and exposure to inhaled droplets was greater for coughing. For both  
943 talking and coughing, the inhaled droplet number followed the same distribution pattern as  
944 the exhaled droplet number shown in Figure 2; the peak value appeared at a smaller droplet  
945 diameter of  $12 \mu\text{m}$ . In contrast, the trend of droplet deposition was totally different.  
946 Compared with inhalation, deposition is more distance-determined, with the deposited droplet  
947 number dropping to almost negligible beyond  $0.3 \text{ m}$  for talking and  $0.8 \text{ m}$  for coughing.  
948 Because larger droplets have a larger Stokes number, it becomes easier for them to be  
949 deposited on the human face. Thus, the number of deposited droplets aggregated at the  
950 medium-large size range. Compared with talking, for coughing the deposition fraction  
951 showed a much slower decay with distance.

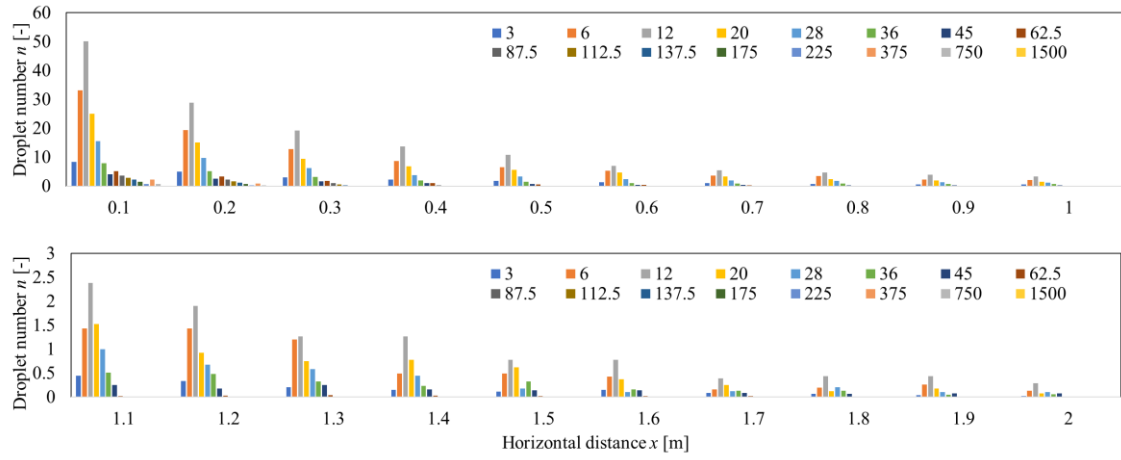
952  
953 It is also worth investigating exactly where the droplets fall. We compare the deposition  
954 number percentage of each facial membrane for  $3 \mu\text{m}$  and  $36 \mu\text{m}$  droplets in Figure B3.  
955 Exhaled droplets began to cover nostrils from  $0.2$  to  $0.3 \text{ m}$  and the eyes from  $0.4$  to  $0.5 \text{ m}$ .  
956 The mouth became less important as the distance increased. Because of the lower exhalation  
957 velocity, the trajectory of the jet curved upward more obviously for talking than for coughing.  
958 Therefore, more droplets deposited onto the eyes at longer distance due to talking. Because  
959 eye protection has been proven to reduce infection via the ocular route, the use of masks with  
960 goggles or a face shield may be a promising policy.

961

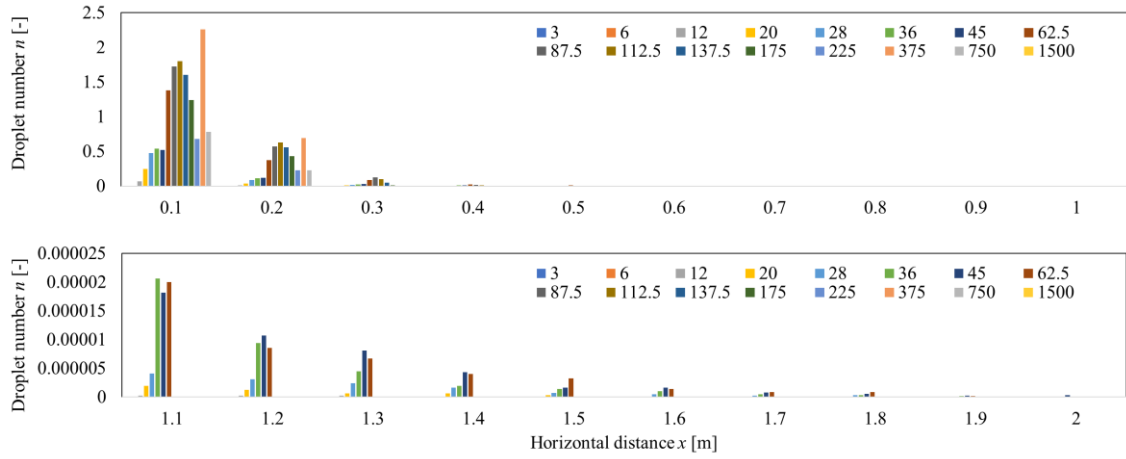


962 **Figure B1.** The calculated membrane fraction (*MF*) and inhalation fraction (*IF*) as a function

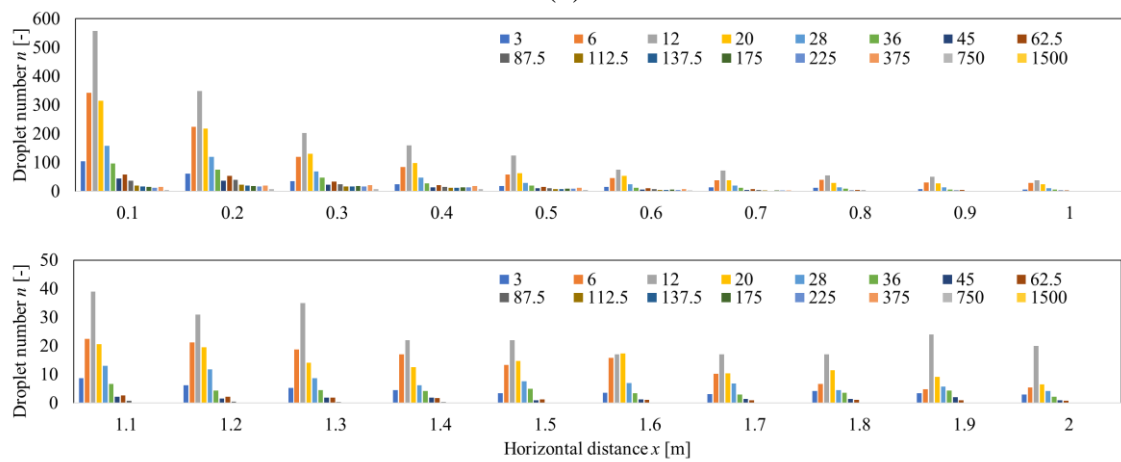
963 of horizontal distance  $x$  and droplet initial size  $d_{do}$ . (a) Talking *MF*; (b) Coughing *MF*; (c)  
 964 Talking *IF*; (d) Coughing *IF*.  
 965



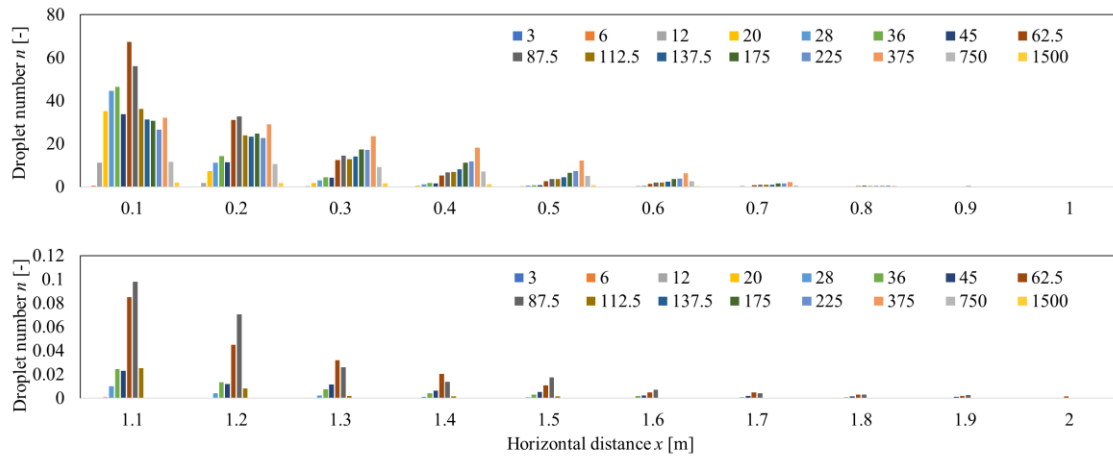
(a)



(b)

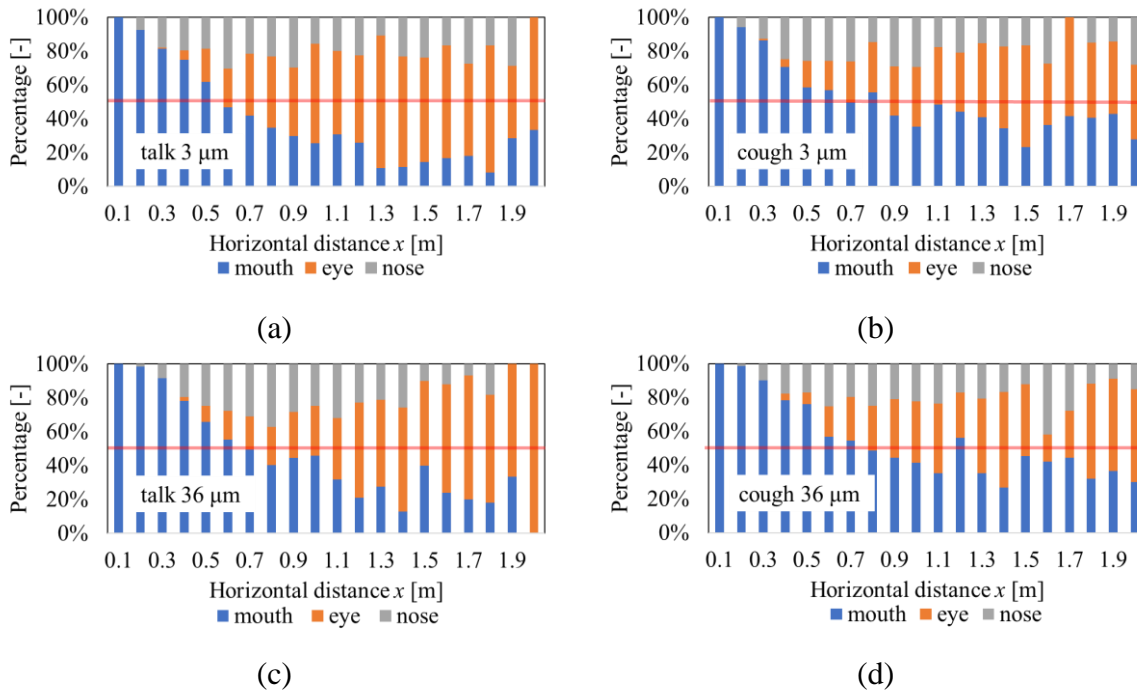


(c)



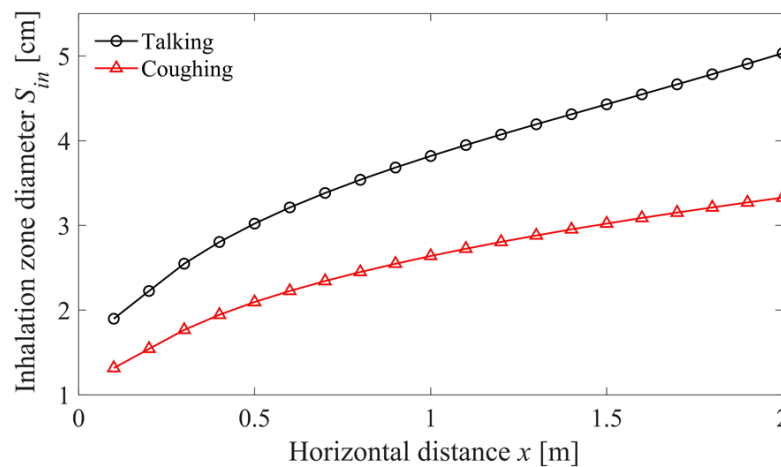
(d)

966 **Figure B2.** Number of inhaled/deposited droplets for talking by (a) Inhalation; (b) deposition  
 967 on facial mucous membranes; and those for coughing by (c) Inhalation; (d) deposition on facial  
 968 mucous membranes.  
 969

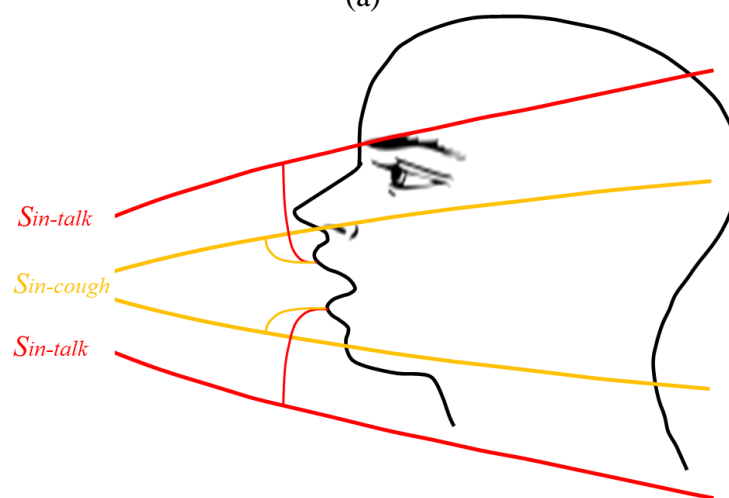


970 **Figure B3.** Percentage of droplet deposition location (a) 3  $\mu\text{m}$  droplets for talking; (b) 3  $\mu\text{m}$   
 971 droplets for coughing; (c) 36  $\mu\text{m}$  droplets for talking; (d) 36  $\mu\text{m}$  droplets for coughing.  
 972





(a)



(b)

973 **Figure B4.** (a) Predicted diameter of the inhalation zone; see Figure 4b. (b) Illustration of  
974 inhalation zone diameter at 1 m relative to the possible location of the mouth opening of the  
975 susceptible person.